의학박사 학위논문

# A study on the pathogenesis of renal fibrosis by Siglec-F-expressing neutrophils

# Siglec-F 발현 호중구에 의한 신장 섬유화 병인 기전 연구

2022년 8월

서울대학교 대학원
의과학과 의과학전공

류 승 원

Ph.D. Dissertation of Medical Science

# Siglec-F 발현 호중구에 의한 신장 섬유화 병인 기전 연구

# A study on the pathogenesis of renal fibrosis by Siglec-F-expressing neutrophils

August, 2022

Seoul National University Graduate School
Department of Biomedical Sciences

Seungwon Ryu

# A study on the pathogenesis of renal fibrosis by Siglec-F-expressing neutrophils

지도 교수 김 혜 영

이 논문을 의학박사 학위논문으로 제출함
2022년 4월

서울대학교 대학원
의과학과 의과학전공
류 승 원

류승원의 의학박사 학위논문을 인준함
2022년 7월

위 원 장 _____ (인)

부위원장 _____ (인)

위 원 _____ (인)

위 원 _____ (인)

위 원 _____ (인)

## ABSRACT

# A study on the pathogenesis of renal fibrosis by Siglec-F-expressing neutrophils

Seungwon Ryu
Department of Biomedical Sciences
Seoul National University Graduate School

Renal injury caused by various conditions usually accompany inflammation. Immune cells from both innate and adaptive immunity contribute to the pathogenic mechanisms of the renal diseases. Chronic unresolved inflammation leads to the renal fibrosis, which is the replacement of the functional tissues with extracellular matrix (ECM) proteins. Because even non-immune mediated renal fibrosis accompanies inflammation, the inflammatory processes are thought to be an important factor in the development of renal fibrosis. Loss of renal function accompanied by the fibrotic changes is generally regarded as irreversible changes. Therefore, the management of underlying renal disease is the key strategy to prevent their progression to renal failure. Given the need for new treatment approaches to manage renal fibrosis, it is crucial to comprehend the pathophysiology of the renal inflammation and/or fibrosis. Until now, most of studies on renal inflammation and fibrosis have been focused on few immune cells

including T cells and macrophages. However, the landscape of renal immune cells is discovered to include various minor innate immune cells.

In this thesis, I aimed to identify the key immune cells involved in the development of renal fibrosis mediated by inflammatory processes (Ryu et al. J Clin Invest. 2022[1]). I discovered that neutrophils were the predominant immune cells in the injured renal tissue caused by unilateral ureteral obstruction (UUO)-induced renal fibrosis model. Abut half of neutrophils that developed in the UUO model expressed Siglec-F, a protein that is normally expressed by eosinophils. Through adoptively transferring and depleting Siglec-F-expressing neutrophils, I demonstrated that Siglec-$F^+$ neutrophils have made a vital role in the development of renal fibrosis. Using intravascular labeling of leukocytes, I found that the development of Siglec-$F^+$ neutrophils was from the infiltrating conventional neutrophils during the injury. Additionally, TGF-β1 and GM-CSF increased during the inflammation and fibrosis were the factor in charge of the conversion of the conventional neutrophils to the Siglec-$F^+$ neutrophils. The mechanisms underlying the function of Siglec-$F^+$ neutrophils in renal fibrosis were dissected in detail, focusing on their direct and indirect contributions to renal fibrosis. First, the indirect contribution was identified from the activation of fibroblasts when cocultured with Siglec-$F^+$ neutrophils, which was derived from the soluble mediators TGF-β1, TNF-α, and IL-1β from Siglec-$F^+$ neutrophils. Additionally, I discovered that Siglec-$F^+$ neutrophils were directly implicated in renal fibrosis via ECM production, especially Collagen 1. These findings demonstrated that the Siglec-$F^+$ neutrophils generated during the renal injury induced progressive renal fibrosis. In summary, I investigated the role of previously unrecognized immune cells during the natural course of renal diseases from renal inflammation to fibrotic

changes. It is expected that a strategy to control Siglec-$F^{+}$ neutrophils leads to the development of a novel therapy for renal disorders associated with fibrosis.

**Keywords:** Renal inflammation, Renal fibrosis, Innate immunity, Neutrophil

***Student Number*:** 2017-39911

* This study included data previously published in The Journal of Clinical Investigation (2022).

# CONTENTS

# LIST OF TABLES

# LIST OF FIGURES

# ABBREVIATIONS

ANOVA: analysis of variance

α-SMA: α-smooth muscle actin

cDNA: complementary DNA

CKD: chronic kidney disease

COL1A1: collagen type 1, alpha 1

CT: control

DAMP: damage-associated molecular pattern

DC: dendritic cell

DN: diabetic nephropathy

ECM: extracellular matrix

ESRD: end stage renal disease

FACS: fluorescence cell sorter

FSC: forward scatter

FSGS: focal segmental glomerulosclerosis

H&E: hematoxylin and eosin

HC: healthy control

i.v.: intravenous

ILC2: type 2 innate lymphoid cell

IRB: institutional review board

IRI: ischemia-reperfusion injury

KO: knock-out

LRRC32: leucine-rich repeat-containing protein 32

mAb: monoclonal antibody

MACS: magnetic activated cell sorting

MCP-1: monocyte chemoattractant protein-1

MT: Masson's trichrome

MDRD: modification of diet in renal disease

NCR: natural cytotoxicity receptor

NET: neutrophil extracellular trap

NGAL: neutrophil gelatinase-associated lipocalin-2

PAS: periodic acid-Schiff

PBS: phosphate buffered saline

PCA: principle component analysis

qPCR: quantitative polymerase chain reaction

RCC: renal cell carcinoma

ROS: reactive oxygen species

RRT: renal replacement treatment

SEM: standard error of the mean

SSC: side scatter

Th: helper T cell

Treg: regulatory T cell

TLR: toll-like receptor

TMR: tissue-resident memory T cell

UUO: unilateral ureteral obstruction

WT: wild-type

# INTRODUCTION

## 1. Renal inflammation and fibrosis

Renal fibrosis is the pathological process of accumulation of extracellular matrix (ECM) proteins in the parenchyma that affects the renal function during renal injuries. Fibrotic change is a typical manifestation of end-stage of a variety of progressive renal diseases. Chronic kidney disease (CKD) is a chronic condition with progressive decrease of renal function that affects approximately 10% of the general population[2, 3]. While hypertension and diabetes are major risk factors of CKD, additional underlying causes such as infection and autoimmune-mediated glomerulonephritis (e.g., lupus nephritis) can contribute to the progressive loss of renal function. Currently, the best therapeutic approaches would be to address these underlying disorders. Because the development of fibrosis usually results in irreversible impairment of renal function, those individuals will eventually proceed to end-stage renal disease (ESRD) requiring renal replacement therapy (RRT) or transplantation. Because RRT is not a cure but is extremely demanding for patients, numerous efforts have been made to find a new therapeutic strategy for progression or prevention of ESRD[4, 5].

Inflammation is commonly found in various renal diseases which lead to the renal fibrosis. It has long been recognized that inflammation has a role in the progression of renal fibrosis[6, 7]. Chronic inflammation is a common finding of CKD, regardless of the etiology. It has long been recognized that inflammation has a role in the development of renal fibrosis. The presence of elevated cytokines and chemokines in patients demonstrates the inflammatory nature of CKD[8, 9, 10]. Various

noxious stimuli, including autoantibodies, toxins, ischemia, and hemodynamic disturbances, activate non-immune cells during the development of renal damage. Endothelial cells, mesangial cells, podocytes, and tubular epithelial cells are all included in the non-immune, intrinsic renal cells. They actively contribute to renal inflammation by generating profibrotic cytokines (TGF-β1, IL-1, IL-4, and IL-6) and growth factors (PDGF and FGF-2). Several studies have shown that when renal cells die, they release damage-associated molecular patterns (DAMPs), which trigger the infiltration of innate immune cells, particularly neutrophils and macrophages [11, 12, 13]. While the pathogenic role of neutrophils in renal fibrosis remains poorly understood, it is possible that these cells directly injure kidney cells by releasing reactive oxygen species and granule contents [14]. They may also indirectly damage renal cells by producing abundant levels of pro-inflammatory mediators that attract and activate other immune cells [15]. When injuries are sustained over an extended period of time, fibrotic mediators accelerate improper tissue regeneration, resulting in an abnormal accumulation of extracellular matrix, leading to the renal fibrosis[16, 17] **(Figure 1)**.

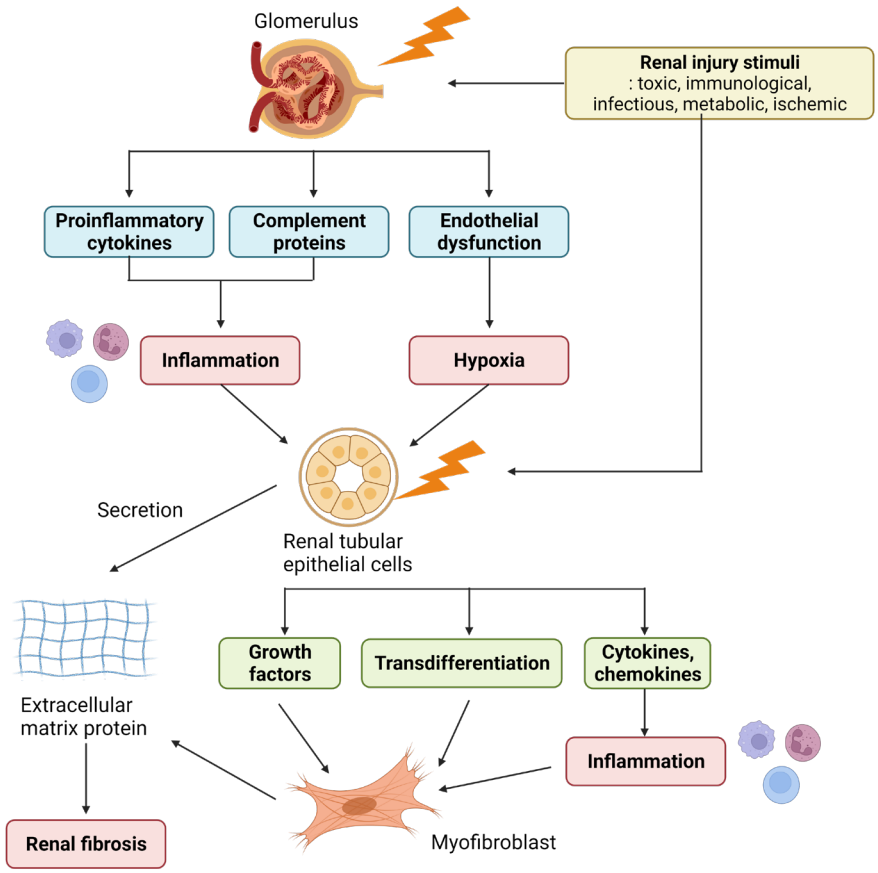


**Figure 1. Mechanism of renal inflammation and fibrosis.**

Fibrosis occurs in the glomerulus (glomerulosclerosis) and/or tubulointerstitium (tubulointerstitial fibrosis) of the kidney. Different noxious stimuli to the renal tissue initiate the inflammatory cascade, which involves the release of cytokines, chemokines, and growth factors by immune and non-immune cells. The release of ECM proteins plays a role in the development of fibrotic tissue changes and kidney failure. (This figure was adapted and modified from Meng et al. Nat Rev Nephrol. 2014[6], and created with Biorender.com.)

## 2. Neutrophil heterogeneity and Siglec-F$^+$ neutrophils

Neutrophils comprise the majority of myeloid populations, which are rapid responders to tissue injuries[18, 19]. Differentiated from the bone marrow progenitors, the circulating neutrophils are infiltrated into the inflamed tissues. The primary role of neutrophils is the elimination of infection and damaged tissues. Their mode of action includes phagocytosis, degranulation, reactive oxygen species (ROS) and cytokine production, and the formation of neutrophil extracellular trap (NET). Although neutrophils are essential to maintain tissue homeostasis, the uncontrolled response of neutrophils could worsen the tissue damage.

Mouse neutrophils are identified as the CD11b$^+$ Ly-6G$^+$ myeloid cells. While they share characteristics cell markers, the diverse subsets are derived from the specific disease conditions[20, 21]. Initially, the concept of pro-tumorigenic (N1) and anti-tumorigenic (N2) neutrophils subsets was proposed, which was termed in parallel with the M1-M2 macrophage paradigm[22]. However, single-cell RNA sequencing reveals that there are eight unique subpopulations of neutrophils in homeostasis and infection[23]. This means that, depending on the specific signals, there may be a more diversified population. By gaining a better understanding of neutrophil heterogeneity, it will be feasible to target certain subsets based on their different functions in disease conditions.

In 2017, it was discovered that a novel subpopulation of neutrophils expressing Siglec-F (Sialic acid-binding immunoglobulin-like lectin F)[24]. Although the function of Siglec-F is unknown, it has been used as a surface marker of eosinophils[25]. Because the conventional methodology for defining neutrophils using flow cytometry excludes the expression of eosinophil marker Siglec-F, the

emergence of Siglec-F$^+$ Ly-6G$^+$ double-positive cells in the lung tumor was unexpected[24]. Examinations of morphology and expression profiles of lung cancer-associated double-positive cells reveal that they are, in fact, neutrophils[26]. Apart from tumor settings, the following investigations have demonstrated that Siglec-F$^+$ neutrophils are generated in variety of inflammatory states, including rhinitis[27], nasal infection[28], myocardial infarction[29, 30], and asthma[31] **(Table 1)**. While they share some properties, such as enhanced ROS production or the development of NETs, their function appears to be context-dependent, depending on the local tissues or disease state. Because our current understanding of Siglec-F$^+$ neutrophils is primarily focused on the respiratory organs, further exploration of this population in other organs is necessary, given their hitherto underappreciated role in neutrophil-dominant inflammatory diseases.

**Table 1.** Studies on Siglec-F-expressing neutrophils

| Tissue | Physiological role | Characteristics | Reference |
|---|---|---|---|
| **Lung tumor** | • Tumor promotion | • Expression of tumor-promoting genes<br>• Increased ROS | Science, 2017[24] |
| **Lung tumor** | • Tumor promotion | • Mature phenotype<br>• Long lived, non-proliferating | Cell Rep, 2020[26] |
| **Olfactory neuroepithelium** | • Neuro-regeneration | • Expression of neurosupportive genes<br>• NET formation | J Leukoc Biol, 2020[27] |
| **Heart** | • Inflammatory during ischemic heart injury | • Higher phagocytic function<br>• Increased ROS | Circ Res, 2020[29]; J Am Heart Assoc, 2021[30] |
| **Nasal epithelium** | • Protective against *Bordetella pertussis* infection | • NET formation | Mucosal Immunol, 2021[28] |
| **Lung** | • Inflammatory during air-pollutant associated asthma exacerbation | • Cysteinyl leukotriene production<br>• NET formation | J Allergy Clin Immunol, 2021[31] |

# 3. Extracellular matrix in renal fibrosis

ECM supports tissue structure by connecting cells together[32]. Excess ECM accumulation, on the other hand, causes pathologic alterations in tissues known as renal fibrosis[33]. Fibrosis may develop in any part of the kidney, including the glomerulus, tubulo-interstitium, and arteries, which corresponds to glomerulosclerosis, tubulo-interstitial fibrosis, and arteriosclerosis or perivascular fibrosis[33]. Although there are multiple pathways that cause fibrosis, TGF-β1 signaling is well-known for its roles in the fibroblast activation and increased ECM deposition, and stiffness[34, 35]. The significance of collagens, particularly Collagen 1, which is the most prevalent ECM protein, has been largely proposed in renal fibrosis[33].

The ECM-producing cells are not only restricted to the fibroblasts, but many cells could contribute to the matrix production. The primary cells responsible for ECM synthesis differ depending on the renal compartment. In the case of tubulo-interstitial fibrosis, which is the endpoint finding of all fibrogenic renal disorders, fibroblasts, myofibroblasts, and pericytes are the primary producers of ECM[33]. Once the fibrosis core has formed, the activated ECM-producing cells may continue to contribute ECM even after the initial harmful stimulus has passed, making intervention in fibrotic disorders difficult[34, 36].

During fibrosis, resident fibroblasts are activated to myofibroblasts. However, it has been reported that myofibroblasts expressing α-smooth muscle actin (α-SMA) can be originated from various cell types other than fibroblasts by the cytokines and mechanical forces[37, 38]. They include pericytes, endothelial cells, tubular epithelial cells, and bone-marrow derived cells[38]. The mechanisms behind

the conversion of each renal cells into the myofibroblasts include as follows: pericytes via differentiation, endothelial cells via endothelial-to-mesenchymal transition, tubular epithelial cells via epithelial-to-mesenchymal transition[37]. Fibrocytes, a circulating CD45+ bone marrow-derived cell subgroup, are an intriguing ECM contributor. They express both myofibroblast-like markers including α-SMA and Collagen 1, and monocyte-like markers including CD11b, CD68, and MHC-II molecules[37]. However, it is still controversial whose origin makes the greatest contribution to the ECM deposition and renal fibrosis.

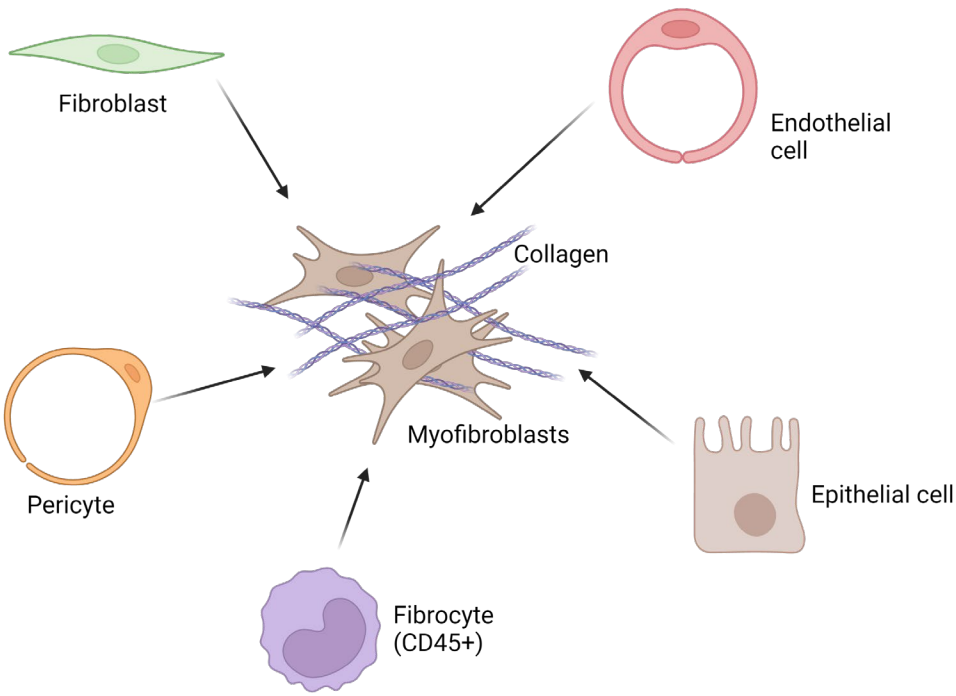


**Figure 3. Origin of extracellular matrix in renal fibrosis.**

Various cell sources in the kidney have been regarded to contribute to the production of extracellular matrix proteins, especially collagen 1. During the renal fibrosis, myofibroblasts are the major contributor in the ECM production. However, other non-immune cells including pericytes, endothelial and epithelial cells are also capable of producing the ECM protein. Recently, the role of bone-marrow derived, $CD45^{+}$ cells, called fibrocytes, are reported to contribute to the renal fibrosis. (This figure was adapted and modified from Mack and Yanagita. Kidney Int. 2015[37], and created with Biorender.com).

# MATERIALS AND METHODS

## Animal models

Six- to ten-week-old male C57BL/6, ΔdblGATA, or Rag1-/- mice were subjected to UUO, IRI, or sham surgery. The UUO model was established by ligating the left ureter with 5-0 silk. Three, seven, or fourteen days after surgery, the kidneys were removed for analysis. To develop renal ischemia-reperfusion injury model, the left renal pedicle was clamped for 30 minutes with a microvascular clamp (Roboz Surgical Instrument). Four- or eight-weeks following surgery, the mice were euthanized. Sham procedures were identical to UUO, Adriamycin therapy, or IRI, with the exception that the ureter or renal artery were not altered, or the animals received PBS instead of Adriamycin. Male BALB/c mice were treated to either UUO surgery or Adriamycin-induced nephropathy at the age of eight weeks. Adriamycin was injected intravenously (11.5 mg/kg mouse weight; Tokyo Chemical Industry) to establish the Adriamycin-induced model. Seven days after induction, the mice were euthanized. All wild-type mice were purchased from Koatech. The Jackson Laboratory supplied the Rag1-/- [B6.129S7-*Rag1*$^{tm1Mon}$/J] and ΔdblGATA [B6.129S1(C)-*Gata1*$^{tm6sho}$/LvtzJ] mice.

All mice in the study were housed in a pathogen-free environment at the Seoul National University Hospital Biomedical Research Institute in Korea. All animal research were authorized by the Institutional Animal Care and Use Committee at Seoul National University Hospital (20-0255).

## Human samples

To assess the clinical implications of findings regarding Siglec-$F^+$ neutrophils in the animal studies, the immune cell populations in healthy and tumor tissues from human patients was analyzed. Seven patients at Seoul National University Hospital who underwent nephrectomy for renal cell cancer donated kidney tissues. The tissues were analyzed by a pathologist and classified as normal or malignant tissue. Additionally, peripheral blood was obtained from two healthy donors. All subjects provided written informed consent. The study protocol was approved by the Seoul National University Hospital Institutional Review Board (2106-081-1226). The bio-specimens were provided by the Seoul National University Human Biobank, which is a member of the National Biobank of Korea and is supported by the Ministry of Health and Welfare, Korea.

## Histology

Formalin-fixed paraffin-embedded tissue blocks were made from mouse kidneys or human biopsy tissues. Before staining, tissue sections (4μm thick) were prepared. The sections were stained with hematoxylin and eosin (H&E), periodic acid-Schiff (PAS), Masson's trichrome (MT), or Sirius red for histological investigation. Collagen 1 levels were evaluated by antigen retrieval and incubation with COL1A1 primary antibody (1:100; Santa-Cruz) followed by horseradish peroxidase-conjugated secondary antibodies (Cell Signaling) according to the manufacturer's instructions. To assess fibrosis in the kidneys, 10 fields were randomly selected and the amount of Sirius red staining and COL1A1 levels were determined under x100 magnification. To evaluate neutrophil morphology,

neutrophils were centrifuged using a cytocentrifuge, fixed in 100% methanol, and stained with Diff-Quik (Sysmex) according to the manufacturer's instructions. Histologic slides were taken and analyzed using a DM750 microscope (Leica) or Axio Scan Z1 (Carl Zeiss) and Leica LasX software (Leica) or Zen Blue software (Carl Zeiss). Immunofluorescence images were obtained using confocal microscopy, FV3000 (Olympus) and analyzed with FV10-ASW 4.0 Viewer (Olympus).

## Tissue protein analysis

Radioimmunoprecipitation assay (RIPA) buffer comprising a protease inhibitor cocktail and EDTA was used to prepare protein from kidney tissues. Total protein was assessed using the bicinchoninic acid (BCA) assay (Thermo Fisher Scientific) and normalized to a concentration of 1–2 mg/mL. 80 g of extracted proteins were run on 8–12 percent gradient gels and transferred to Immobilon Polyvinylidene difluoride membranes for Western blot analysis (Merck Millipore). Immunoblotting was performed using the following antibodies: NGAL (1:100, Santa Cruz, SC-515876), P16 (1:500, Sigma-Aldrich, LS-B5261), COL1A1 (1:1000, Novus, NBP1-30054), α-SMA (1:1000, Abcam, ab32575), fibronectin (1:500, Abcam, ab2413), Snail (1:400, Abcam, ab180714) (1:5000, Sigma-Aldrich, 14c10). Gel documentation system was used to acquire the images (Gel Doc 1000, Bio-Rad). ImageJ software was used to quantify protein bands from Western blots (NIH). To identify the proinflammatory cytokines that converts conventional neutrophils to Siglec-$F^{+}$ neutrophils, a bead-based immunoassay was performed according to the manufacturer's instructions (LEGENDplex$^{TM}$ mouse inflammation

panel and active/total TGF-β1 assay, Biolegend). The result of array was examined using a BD LSRFortessa X-20 flow cytometer (BD Biosciences) and the manufacturer's Legendplex web-based software (https://legendplex.qognit.com).

## Human/mouse kidney leukocyte isolation

Whole kidneys from experimental mice were prepared in cold PBS, as were sections of nephrectomized kidneys from patients. Using a scalpel blade, tissues were mechanically fragmented into tiny pieces. To further disintegrate the cells, the tissues were enzymatically digested for 45 minutes at 37°C with 1 mg/mL collagenase IV (Worthington Biochemical) and 50 g/mL DNase I (Sigma-Aldrich). The cells were then filtered and washed with cold PBS using 40μm strainers. After resuspending the cell pellet in 40% Percoll solution (GE Healthcare), it was placed on top of 80% Percoll solution. After centrifugation at 2000 rpm for 4°C, the leukocyte layers between the two Percoll solutions were recovered. Leukocytes were washed with PBS for further investigation.

## Human neutrophil isolation from peripheral blood

Human blood was diluted to 1:1 ratio with PBS. Diluted blood was layered on top of the Histopaque-1077 (Sigma-Aldrich) and Histopaque-1119 (Sigma-Aldrich) solutions. After centrifugation at 700xg for 4°C, the layer on top of the bottom red fragments were recovered. Neutrophils were washed with PBS for further investigation.

## Flow cytometric analysis and cell sorting

Mouse or human cell preparations were resuspended in PBS and treated for 10 minutes with Zombi-Aqua viability dye (Biolegend) and mouse or human Fc block (BD Biosciences). After the washing step, the cells were resuspended in FACS buffer (PBS with 2% FBS) and treated for 30 minutes with the following FITC-, PerCP-Cy5.5-, PE-Cy7-, PE-, APC-, BV421-, BV650-, or BV785-conjugated mouse or human monoclonal antibodies. The mouse antibodies were specific for I-Ab (AF6-120.1, Biolegend), Ly-6G (1A8, Biolegend), Siglec-E (M1304A01, Biolegend), CCR3 (J073E5, Biolegend), CD11c (HL3, BD Biosciences), CD11b (M1/70, Biolegend), F4/80 (BM8, Biolegend), Siglec-F (S17007L, Biolegend), CD19 (1D3, BD Biosciences), CD3e (145-2C11, Biolegend), NK1.1 (PK136, Biolegend), CD8a (53-6.7, Biolegend), CD90.2 (30-H12, Biolegend), CD25 (PC61, Biolegend), CD4 (RM4-5, Biolegend), and CD45 (30-F11, Biolegend). The human antibodies were specific for CD14 (HCD14, Biolegend), CD15 (W6D3, Biolegend), Siglec-8 (7C9, Biolegend), CD16 (3G8, Biolegend), and CD45 (HI30, Biolegend). For the Annexin V assays, cells were incubated in Annexin V buffer containing Annexin V for 30 minutes and then evaluated within 30 minutes according to the manufacturer's instructions. Cells were fixed and permeabilized according to the manufacturer's instructions for the proliferation and intracellular staining experiments using the eBioscience Foxp3/Transcription factor labeling kit (Invitrogen). The cells were then stained with Ki-67 (Biolegend), COL1A1 (polyclonal, Rockland Immunochemicals) for an hour in Foxp3/Transcription factor staining buffer. To evaluate intracellular cytokines, cells were restimulated for 3 hours with 100 ng/mL LPS (Merck).

Following fixation and permeabilization with the BD Cytofix/Cytoperm kit (BD Biosciences), the cells were treated with antibodies specific for TGF-β1 (TW7-16B4), TNF-α (MP6-XT22, Invitrogen), and IL-1β (NJTEN3, BD Biosciences). The BD LSRFortessa X-20 flow cytometer (BD Biosciences) was used to evaluate the samples, and the results were analyzed using the FlowJo v10.6.1 software (BD Biosciences). The cells were sorted using a BD FACSAria III after the staining steps described above (BD Biosciences). The supplier was described only when it was not from Biolegend.

## Real-time quantitative PCR

TRIzol reagent (Invitrogen) was used to extract RNA from tissues or sorted cells according to the manufacturer's instruction. Complementary DNA (cDNA) was synthesized using the SensiFAST cDNA synthesis kit from 1 μg of RNA (Bioline). The cDNA was utilized as templates for quantitative polymerase chain reaction (qPCR) with the SensiFAST™ SYBR Lo-ROX or Probe Lo-ROX kits (Bioline). qPCR was done according to the manufacturer's instructions using the Bio-Rad CFX96™ Real-Time PCR Detection System. The expression level of interest genes was normalized by *GAPDH*. All primers used in the procedures were purchased from Integrated DNA Technologies **(Table 2)**.

**Table 2.** Primer sequences for RT-qPCR

| Gene | Forward primer | Reverse primer |
|---|---|---|
| *Il1b* | TCGCTCAGGGTCACAAGAAA | CATCAGAGGCAAGGAGGAAAAC |
| *Tnfa* | GGTGCCTATGTCTCAGCCTCTT | GCCATAGAACTGATGAGAGGGAG |
| *Tgfb1* | TTGCCGAGGGTTCCCGCTCT | CCTCCCGGGCGTCAGCACTA |
| *Col1a1* | CCTGGTAAAGATGGTGCC | CACCAGGTTCACCTTTCGCACC |

## Intravascular leukocyte labeling

To differentiate immune cells in the renal vasculatures from those in the renal parenchyma, mice were anesthetized with isoflurane and intravascularly injected with BV650-labeled anti-mouse CD45 monoclonal antibodies 5 minutes before euthanasia, according to the past protocol[39].

## Depletion of Siglec-F$^{+}$ neutrophils

To investigate the involvement of Siglec-F$^{+}$ neutrophils in renal fibrosis, UUO mice were depleted of these cells using Siglec-F or Ly-6G depletion antibodies. Mice were intraperitoneally injected with the isotype antibody (40 g/200 L PBS; KLH, R&D Systems), the Siglec-F depletion antibody (40 g/200 L PBS; Q920G3, R&D Systems), or the Ly-6G depletion antibody (400 g/200 L; 1A8, BioXCell) on days 2 and 4 following UUO surgery. Flow cytometric analysis was used to determine the extent to which the treatments depleted the cells.

## Conversion of neutrophils in vitro and coculture with fibroblasts

Using the magnetic-activated cell sorting (MACS) kit (Miltenyi Biotech) for mouse or human neutrophils, neutrophils were concentrated from naive mouse bone marrow or human blood. Neutrophils ($1x10^5$ cells/well) were cultured overnight in RPMI1640 media with 10% FBS and 10 ng/mL of the recombinant proteins IL-23 (Biolegend), MCP-1 (Biolegend), TGF-β1 (Biolegend), and/or GM-CSF (Biolegend). After washing the cells with PBS, the cells were examined for

Siglec-F expression using flow cytometry and COL1A1 expression using ELISA (Cusabio Technology) and immunofluorescence imaging.

For the co-culture experiment, $3x10^5$ NIH3T3 fibroblasts (ATCC) per well were plated in a 6-well plate and cultured for one day prior to co-culture in serum-starved RPIMI 1640 medium. After priming neutrophils in vitro with TGF-β1 or GM-CSF, they were co-cultured with fibroblasts at 1:10 ratios. After 24 hours of co-culture, the neutrophils were washed three times with PBS and the fibroblast lysates were used for Western blot analysis to determine the levels of COL1A1 and α-SMA.

## Adoptive transfer of Siglec-$F^+$ neutrophils

Siglec-$F^+$ neutrophils were generated via in vitro conversion of bone marrow derived neutrophils with TGF-β1 and GM-CSF, as described above. After 3 or 10 days of UUO, $1x10^6$ Siglec-$F^+$ neutrophils were intravenously administered into control or UUO mice. At day 14 of UUO, all mice were euthanized for histological examination, Western blot, and RT-PCR.

## Statistics

The results were reported as mean ± standard error of the mean. Depending on the normality, groups were compared using paired/unpaired Student's t-test, Mann-Whitney U test, Wilcoxon rank sum test, or one-way analysis of variance (ANOVA) followed by Dunnett's post hoc test. Pearson's or Spearman's correlation tests were used to conduct correlation analysis on parametric or nonparametric data, respectively. The significance level (*P*-value)

was 0.05 for two-tailed tests. GraphPad Prism 9 was used for statistical analysis (GraphPad).

# RESULTS

## Neutrophils accumulate during UUO-induced renal fibrosis

The unilateral ureteral obstruction (UUO) model is induced by the surgical ligation of the left ureter **(Figure 4)**. It is a commonly used animal model for CKD, in part because of its rapid induction of renal fibrosis[40]. As demonstrated by Periodic Acid Schiff, Masson's trichrome, Sirius red, and collagen type 1, alpha 1 (COL1A1) staining, it promotes both tubular cell death and renal fibrosis. These events, in turn, result in substantial hydronephrosis and parenchymal loss in the kidney **(Figure 5)**. These alterations are followed by an increase in renal injury markers throughout time, including neutrophil gelatinase-associated lipocalin-2 (NGAL), P16, α-smooth muscle actin (α-SMA), and COL1A1 **(Figure 6)**.

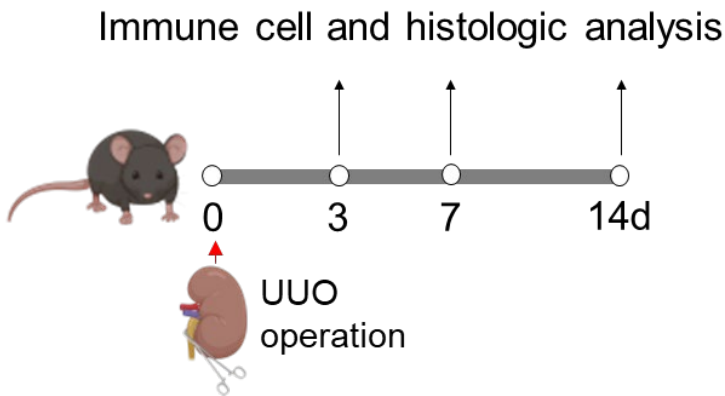


**Figure 4. UUO induced renal fibrosis model.**

C57BL/6 mice underwent unilateral ureteral obstruction (UUO) surgery, after which the fibrosis and immune cell profiles in the kidneys were evaluated on postoperative days 0, 3, 7, and 14. The figure was created with icons from Biorender.com.

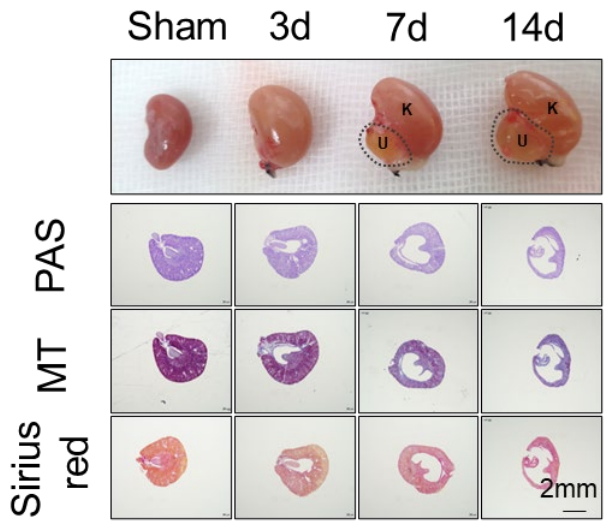


**Figure 5. Establishment of UUO induced renal fibrosis model shown by histologic evaluation.**

C57BL/6 mice underwent unilateral ureteral obstruction (UUO) surgery, after which the fibrosis and immune cell profiles in the kidneys were evaluated on postoperative days 0, 3, 7, and 14. Images of the whole harvested kidneys and Periodic Acid Schiff (PAS), Massons' trichrome (MT), and Sirius red staining. U: ureter, K: kidney.

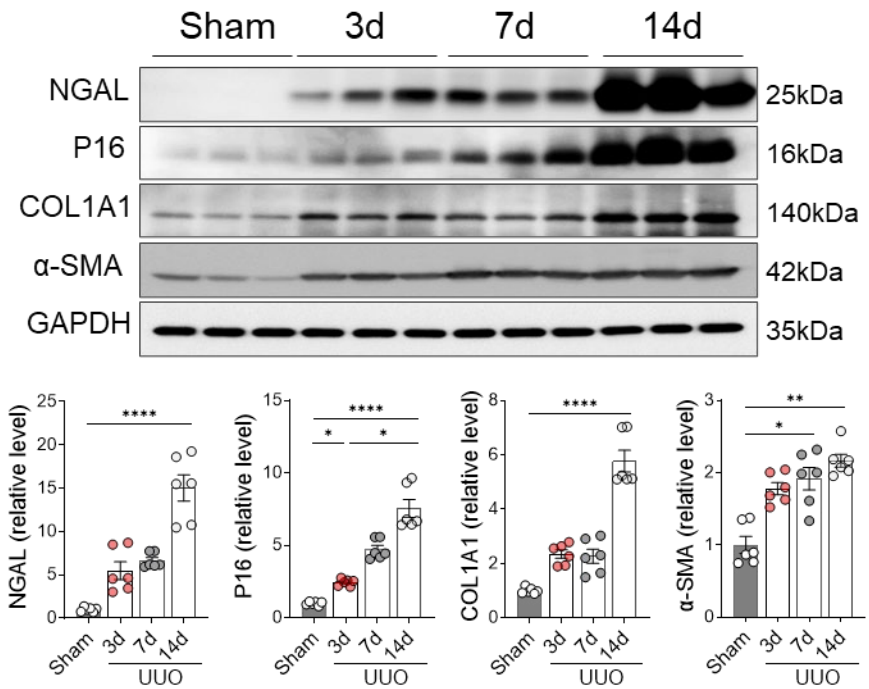


**Figure 6. Establishment of UUO induced renal fibrosis model shown by renal injury markers.**

C57BL/6 mice underwent unilateral ureteral obstruction (UUO) surgery, after which the fibrosis and immune cell profiles in the kidneys were evaluated on postoperative days 0, 3, 7, and 14. Evaluation of renal damage and fibrosis by Western blot analysis NGAL, P16, α-SMA and COL1A1. All results are shown as mean ± SEM and statistical analysis was performed using one-way ANOVA test. **P*<0.05; ***P*<0.01; *****P*<0.0001; n = 5-7 mice in each group.

When I performed flow cytometric analyses on the immune cell profiles of UUO-injured kidneys, I discovered that the frequency of $CD45^+$ leukocytes rose significantly as renal fibrosis progressed **(Figure 7)**. However, lymphocytes (the $SSC^{low}FSC^{low}$ population) declined dramatically in frequency **(Figure 8)**. A detailed assessment of the $CD45^+$ leukocyte subsets revealed that T cells, B cells, natural killer cells, and type 2 innate lymphoid cells (ILC2s) were all decreased in their frequencies following UUO **(Figures 9 amd10)**. By contrast, when I examined granulocytes, I discovered that the frequency of neutrophils increased dramatically as renal fibrosis progressed (but not of eosinophils, macrophages, or dendritic cells) **(Figure 10)**. Thus, because renal immune cell profiling revealed that neutrophils are the most frequent immune cell population in kidneys with severe fibrosis, this cell type may play a role in UUO pathogenesis.

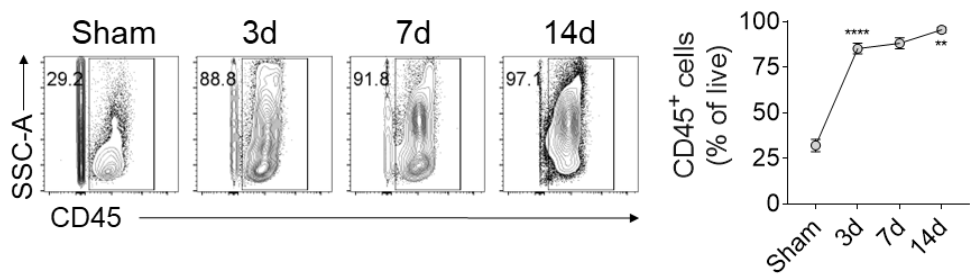


**Figure 7. CD45$^+$ immune cell changes by UUO induced renal injury.**

Frequency of CD45$^+$ leukocytes and lymphocytes during UUO induced injury were analyzed with flow cytometry. All results are shown as mean ± SEM and statistical analysis was performed using one-way ANOVA test. *$P$<0.05; **$P$<0.01; ****$P$<0.0001; n = 5-7 mice in each group.

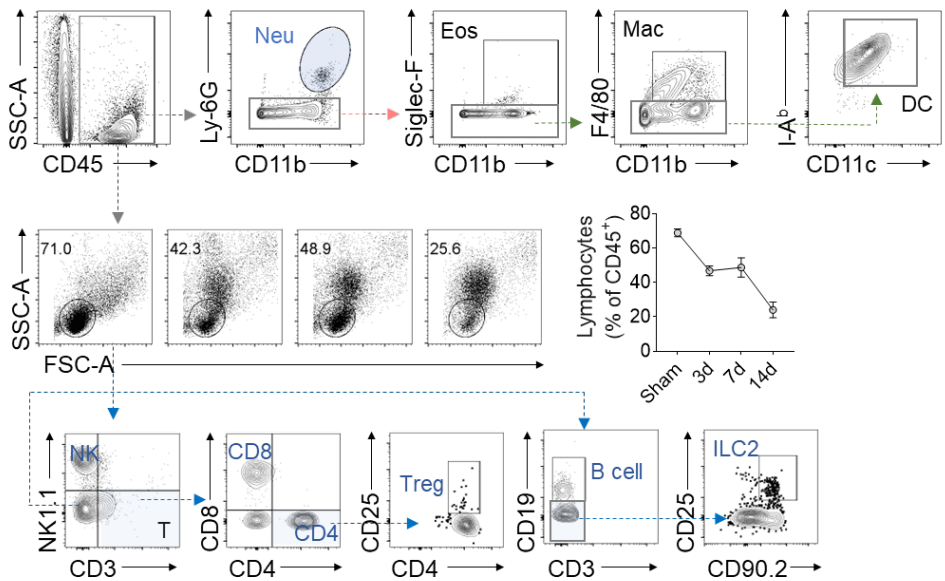


**Figure 8. Gating strategy of renal immune cells.**

Profiling of renal immune cells delineated total T cells, $CD4^+$, $CD8^+$ T cells, regulatory T cells ($CD4^+$ $CD25^+$), NK cells, B cells, and ILC2s ($CD3^-$ $CD19^-$ $NK1.1^-$ $CD90.2^+$ $CD25^+$) during UUO-induced renal injury. All results are shown as mean ± SEM. n = 5-7 mice in each group.

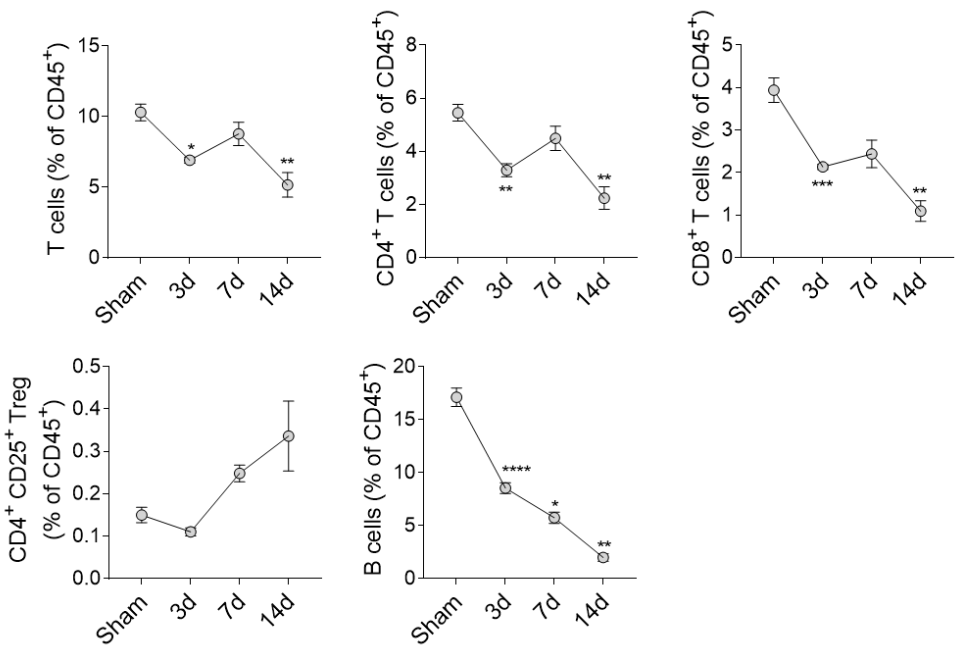


**Figure 9**. **Adaptive immune cell profiling of UUO-induced renal injury.**

Frequencies of adaptive immune cells including T cells, $CD4^+$, $CD8^+$ T cells, regulatory T cells (Treg), and B cells. All results are shown as mean ± SEM and statistical analysis was performed using one-way ANOVA test. **P*<0.05; ***P*<0.01; ****P*<0.001; *****P*<0.0001; n = 5-7 mice in each group.

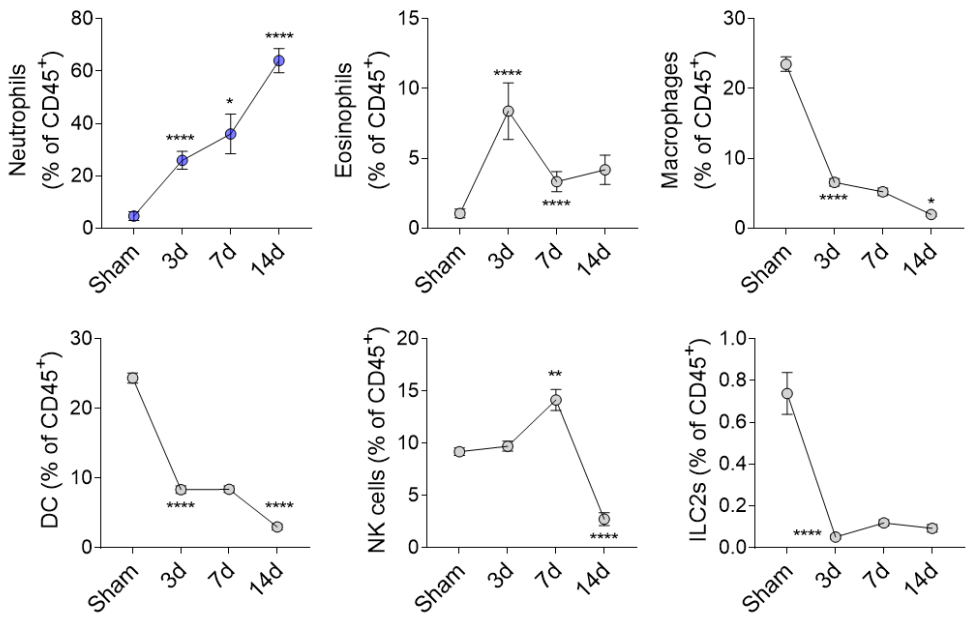


**Figure 10**. **Innate immune cell profiling of UUO-induced renal injury.**

Frequencies of granulocytes including neutrophils, eosinophils, macrophages, DCs, NK cells, and ILC2s. All results are shown as mean ± SEM and statistical analysis was performed using one-way ANOVA test. **P*<0.05; ***P*<0.01; ****P*<0.001; *****P*<0.0001; n = 5-7 mice in each group.

## Novel Siglec-F-expressing neutrophils accumulate in UUO-injured kidneys

When I examined the surface markers of neutrophils in fibrotic kidneys in further detail, I discovered an unexpectedly large population of Ly-6G$^{+}$ neutrophils that co-expressed the eosinophil-specific surface marker Siglec-F **(Figure 11A)**. A kinetic study next revealed that these Siglec-F$^{+}$Ly-6G$^{+}$ cells were exceedingly rare in the kidney at baseline but increased to 24 percent of CD45$^{+}$ leukocytes after 14 days as inflammation and fibrosis proceeded in the UUO-injured kidney **(Figure 11B)**. Conventional neutrophils (Siglec-F$^{-}$Ly-6G$^{+}$) also increased significantly following UUO, from 5% of CD45$^{+}$ leukocytes at baseline to 42% at 14 days **(Figures 11B and 12)**. This difference was evident regardless of whether UUO was performed on C57BL/6 or BALB/c mice **(Figure 13)**.

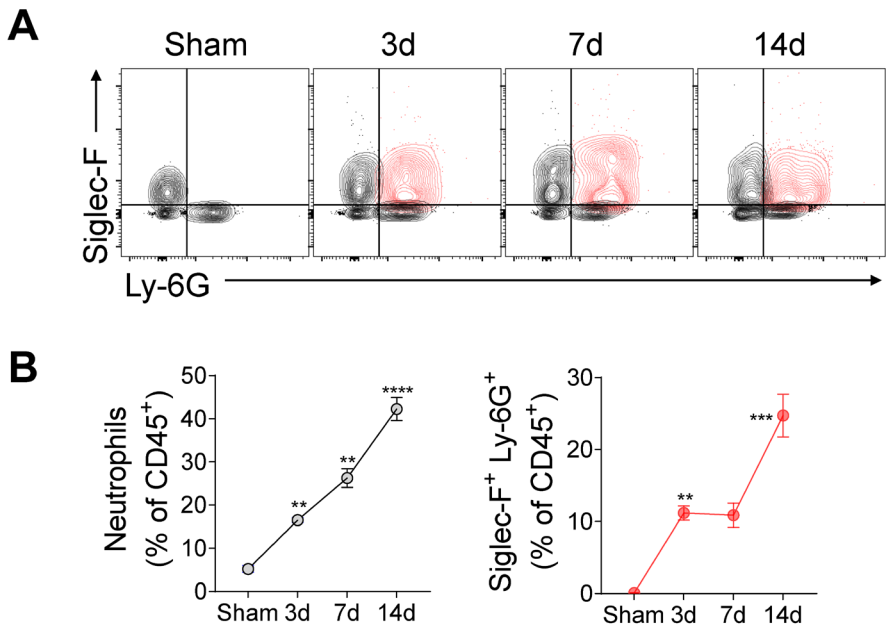


**Figure 11**. **Emergence of Siglec-F-expressing neutrophils in fibrotic kidney.**

Representative flow cytometry dot plot (A) and bar graphs showing the emergence of Siglec-F$^{+}$ Ly-6G$^{+}$ cells during the UUO-induced injury. All results are shown as mean ± SEM and statistical analysis was performed using one-way ANOVA test. **P<0.01; ***P<0.001; ****P<0.0001; n = 4-5 mice in each group.

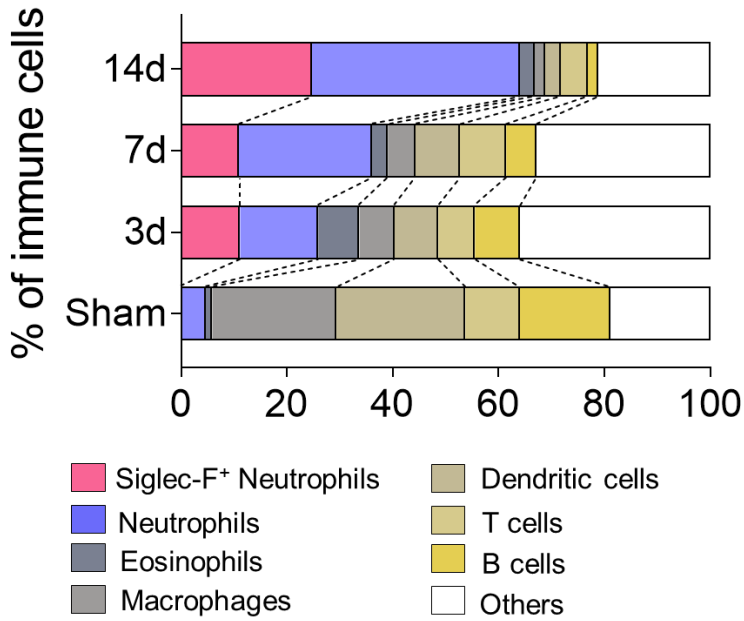


**Figure 12. Changes in the immune cell landscapes during the UUO induced injury.**

The composition of major immune cells in kidneys was compared during the time-course of UUO-induced injury from day 0 to day 14 following the surgery. All results are shown as mean ± SEM. n = 4-5 mice in each group.

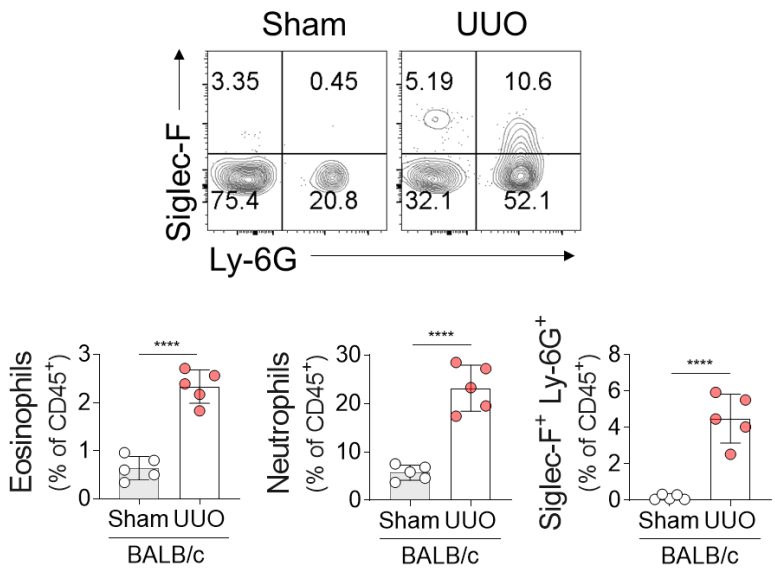


**Figure 13**. **Emergence of Siglec-F-expressing neutrophils regardless of mouse strains.**

The Siglec-F-expressing neutrophils were identified in the BALB/c-background fibrotic kidney. All results are shown as mean ± SEM and statistical analysis was performed using Mann-Whitney test. ****P<0.0001; n = 5 mice in each group.

Our phenotypic study of neutrophils revealed that both the newly identified Siglec-$F^{+}Ly\text{-}6G^{+}$ cells and conventional neutrophils displayed the neutrophil marker Siglec-E but not the eosinophil marker CCR3, whereas eosinophils expressed Siglec-F and CCR3 but not Siglec-E or Ly-6G **(Figure 14)**. Additionally, our morphological examination revealed that the new cells had multilobulated characteristics similar to those of conventional neutrophils. Notably, the novel population contained a greater proportion of hyper-segmented cells and showed higher size as shown by the FSC-A **(Figures 15 and 16)**. Notably, Ogawa et al. demonstrated that Siglec-$F^{+}$ neutrophils co-express the macrophage marker F4/80 in inflamed olfactory neuroepithelium[27]. The unique cells I observed, however, did not exhibit the macrophage marker F4/80, indicating they were not contaminated with renal macrophages **(Figure 17)**.

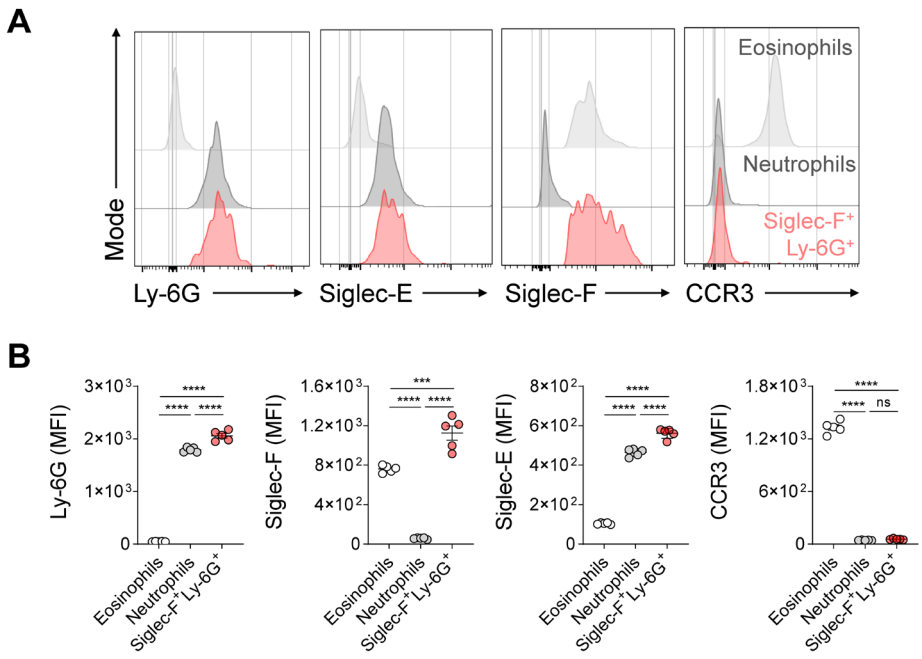


**Figure 14. Characteristics of Siglec-F$^+$ Ly-6G$^+$ cells examined by the expression of neutrophil and eosinophil markers.**

Siglec-F$^+$ Ly-6G$^+$ cells were compared with conventional neutrophils and eosinophils for the expression of Ly-6G, Siglec-E, Siglec-F, and CCR3. All results are shown as mean ± SEM and statistical analysis was performed using one-way ANOVA test. ***P<0.001; ****P<0.0001; n = 5 mice in each group. ns, not significant; MFI, mean fluorescence intensity.

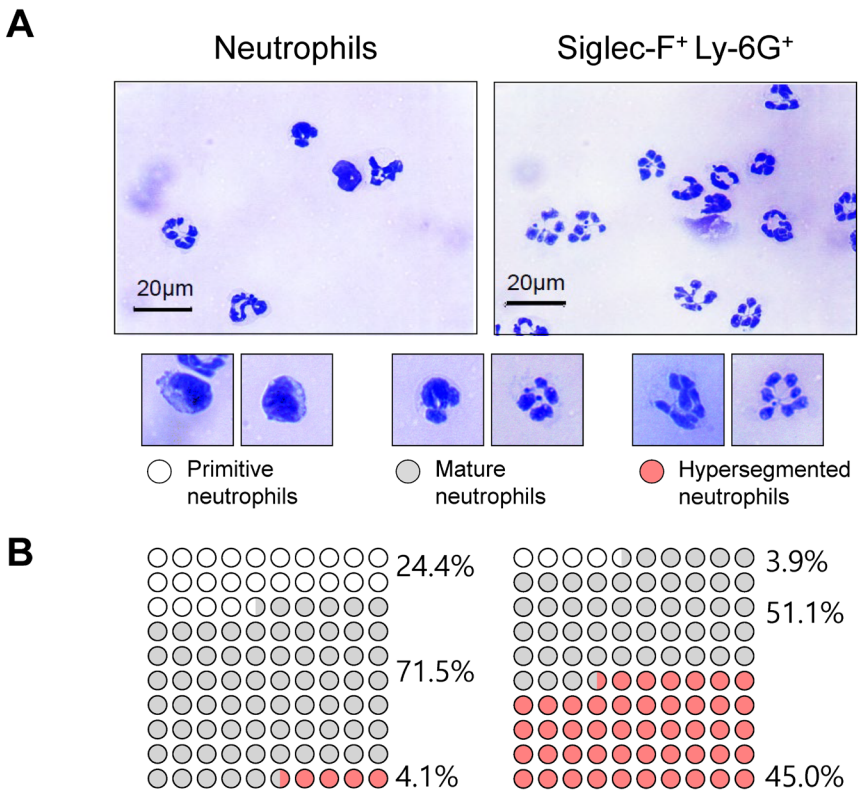


**Figure 15. Comparison of morphologies between neutrophils and Siglec-F$^+$ Ly-6G$^+$ cells.**

(A) Evaluation of the morphology of the conventional neutrophils and the novel Siglec-F$^+$Ly-6G$^+$ cells on day 14 by sorting and staining them with Diff-quick and (B) counting the numbers of primitive, mature, and hypersegmented neutrophils.

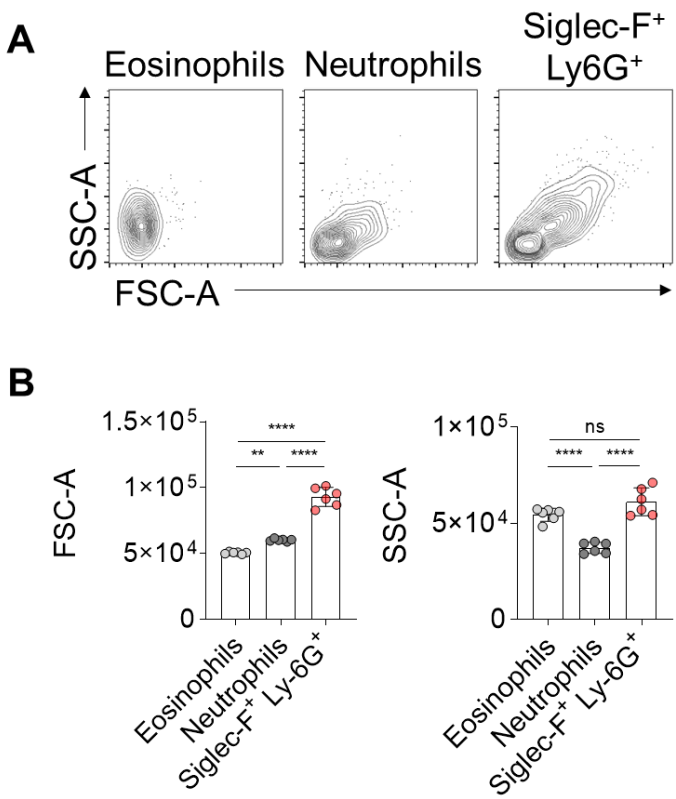


**Figure 16. Comparison of FSC and SSC between neutrophils and Siglec-F$^+$ Ly-6G$^+$ cells.**

Siglec-F$^+$ Ly-6G$^+$ cells were compared with conventional neutrophils and eosinophils for FSC and SSC by flow cytometry. All results are shown as mean ± SEM and statistical analysis was performed using one-way ANOVA test. **P<0.01; ****P<0.0001; n = 6-7 mice in each group. ns, not significant.

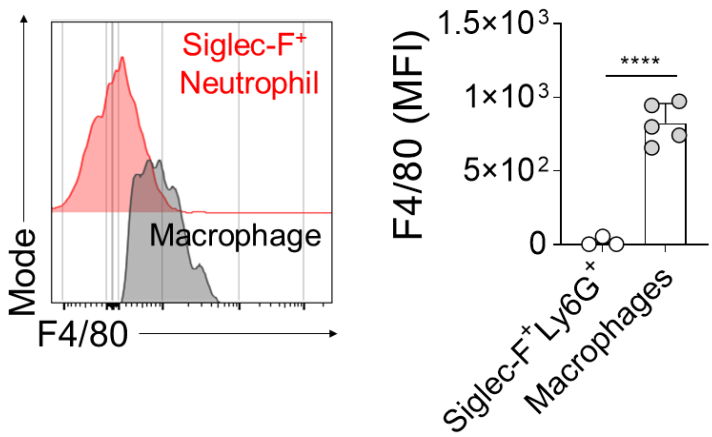


**Figure 17**. **F4/80 expression in Siglec-F$^+$Ly-6G$^+$ cells and macrophages.**

Siglec-F$^+$ Ly-6G$^+$ cells were compared with macrophages for F4/80 expression by flow cytometry. All results are shown as mean ± SEM and statistical analysis was performed using Student's t tests. ****P<0.0001; n = 3-5 mice in each group.

To ascertain that the neutrophils expressing Siglec-F were indeed distinct from eosinophils, I injected mice with recombinant IL-33 on days 0, 1, 2, and 3 following UUO **(Figure 18)**. IL-33 induced eosinophil expansion[41]: if the novel population is an eosinophil population, the treatment will result in their expansion in the kidney. While IL-33 therapy greatly raised eosinophil frequencies, it had no effect on the Siglec-$F^+$Ly-$6G^+$ population **(Figure 19)**. Furthermore, UUO could generate the Siglec-$F^+$Ly-$6G^+$ population in eosinophil-deficient ΔdblGATA mice **(Figure 20A)**. On day 14, the ΔdblGATA mice and their control BALB/c mice exhibited comparable Siglec-$F^+$Ly-$6G^+$ cell frequencies (6% vs. 4%) **(Figure 20B)**. Together, these findings established that Siglec-$F^+$Ly-$6G^+$ cells are neutrophils, but they differ from conventional neutrophils in terms of Siglec-F expression, hypersegmentation, size, and granularity. This population will hereafter be referred to as Siglec-$F^+$ neutrophils.

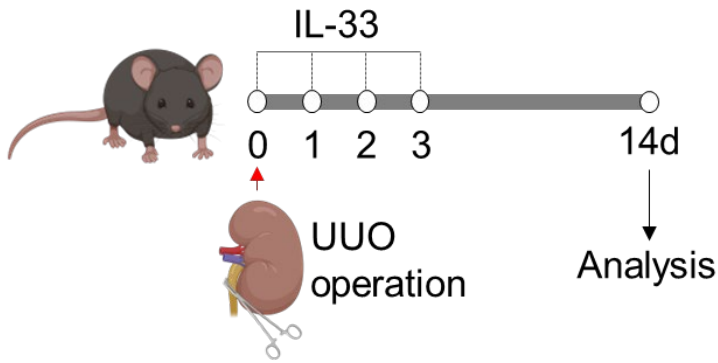


**Figure 18**. **Experimental scheme of IL-33 treatment during UUO-induced renal injury.**

Mice were treated with the recombinant IL-33 (250 ng) for four consecutive days starting on the day of UUO surgery and analyzed on day 14. The figure was created with icons from Biorender.com.

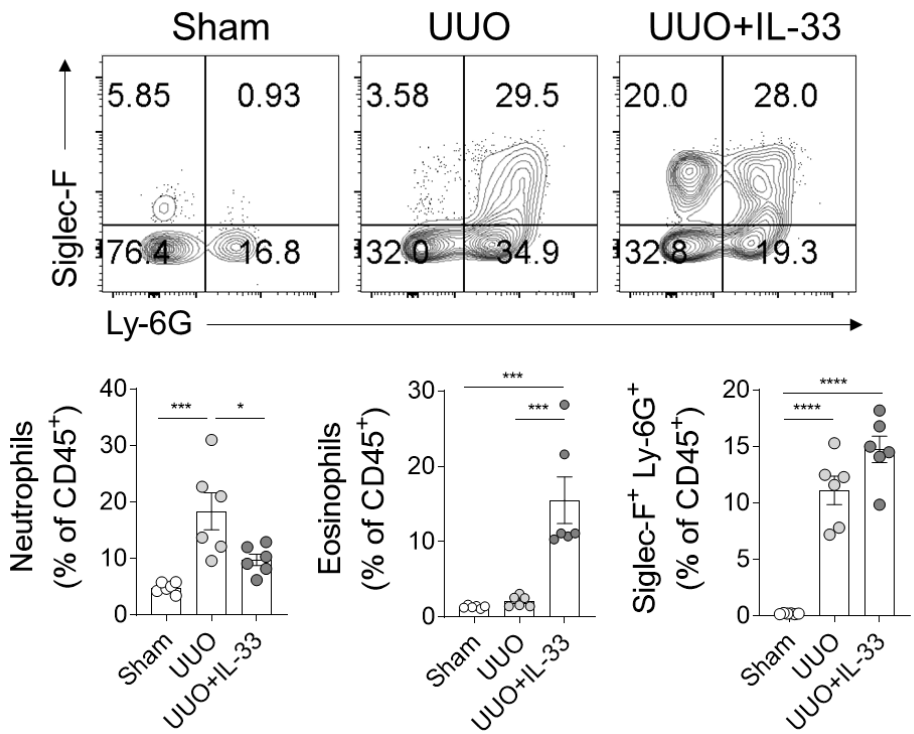


**Figure 19**. **IL-33 treatment during UUO-induced renal injury.**

Mice were treated with the recombinant IL-33 (250 ng) for four consecutive days starting on the day of UUO surgery and the frequencies of conventional neutrophils, eosinophils, and novel Siglec-F$^{+}$Ly-6G$^{+}$ cells on day 14 were determined by flow cytometry. All results are shown as mean ± SEM and statistical analysis was performed using one-way ANOVA test. *P<0.05; ***P<0.001; ****P<0.0001; n = 4-6 mice in each group.

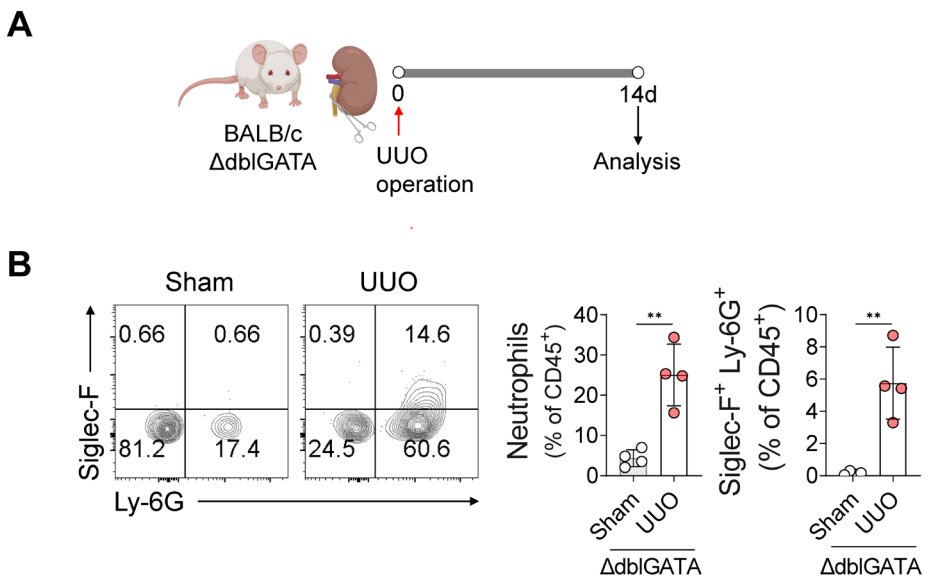


**Figure 20. UUO induced renal injury in the eosinophil-deficient ΔdblGATA mice.**

Eosinophil-deficient ΔdblGATA mice (BALB/c background) were subjected to UUO (A) and the conventional neutrophil and Siglec-F$^{+}$Ly-6G$^{+}$ cell frequencies in the kidney on day 14 were determined by flow cytometry (B). The figure (A) was created with icons from Biorender.com. All results are shown as mean ± SEM and statistical analysis was performed using Mann-Whitney test. **P<0.01; n = 4 mice in each group.

## UUO-induced Siglec-F$^+$ neutrophils are localized in the damaged kidney and arise from conventional neutrophils in the renal vasculature

To determine the origin of the Siglec-F$^+$ neutrophils in the fibrotic kidney, I examined the peripheral blood, spleen, bone marrow, and contralateral kidney of sham- and UUO-induced mice. In both sham- and UUO-induced mice, Siglec-F$^+$ neutrophils were barely detectable in peripheral blood, spleen, and bone marrow. However, only in the injured left kidney, Siglec-F$^+$ neutrophils accounted for 15.4 percent of CD11b$^+$ myeloid cells (0.27 percent in the left kidney of the sham-treated mice). By contrast, in UUO mice, conventional neutrophils still increased in the peripheral blood and spleen **(Figure 21)**. The latter observation is consistent with the prevalent view of CKD as a systemic disease[42]. As a result, I postulated that Siglec-F$^+$ neutrophils were converted from conventional neutrophils in inflammatory renal lesions, rather than being recruited in its mature form.

To investigate this hypothesis, I first examined the proliferation of Siglec-F$^+$ and conventional neutrophils with Ki-67 staining. While 22% of conventional neutrophils were proliferating at baseline, this dramatically decreased to a low of 3% on day 14. On day 7, the Siglec-F$^+$ neutrophils had a very slight increase in proliferative activity, which thereafter declined to very low levels on day 14. Thus, neither population exhibited a high rate of proliferation **(Figure 22)**. Additionally, I observed that, whereas conventional neutrophils exhibited a low but increasing level of apoptotic activity over time, Siglec-F$^+$ neutrophils soon developed a high level of apoptotic activity **(Figure 23)**. These findings suggest that the increase in the Siglec-F$^+$ neutrophil population in the damaged kidney (as shown in **Figure 11**)

is due to continuous replenishment of these cells, but not from proliferating Siglec-$F^+$ neutrophils; rather, the Siglec-$F^+$ neutrophils appear to be generated from conventional neutrophils.

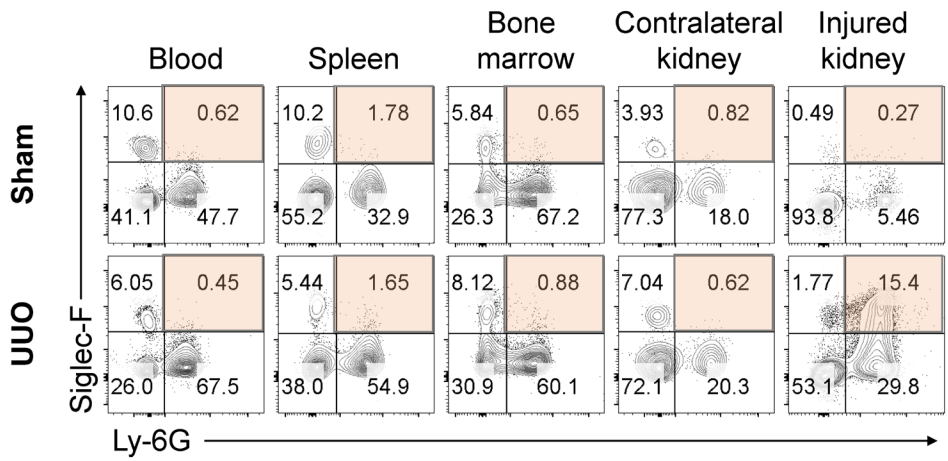


**Figure 21**. **Siglec-F$^{+}$ neutrophils localized to the injured kidneys.**

Flow cytometric analysis of the frequencies of Siglec-F$^{+}$ neutrophils in other organs (blood, spleen, bone marrow, and the contralateral kidney) as well as the injured kidney in UUO-treated mice on day 7.

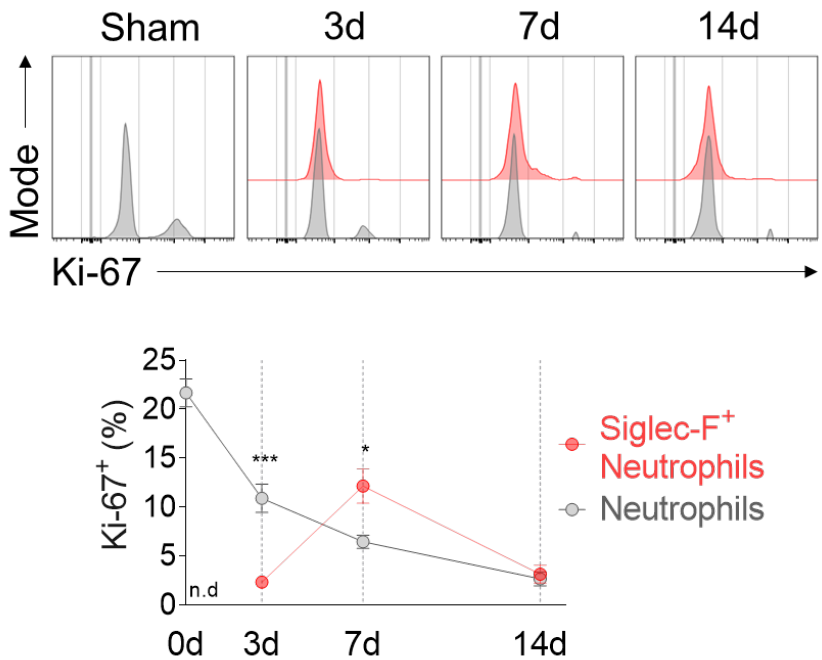


**Figure 22**. **Proliferation of Siglec-F$^{+}$ neutrophils.**

Kinetic changes of the Siglec-F$^{+}$ and conventional neutrophil frequencies in terms of cell proliferation (Ki-67 staining). All results are shown as mean ± SEM and statistical analysis was performed using Mann-Whitney test. *P<0.05; ***P<0.001; n = 4-5 mice in each group. n.d.: not detected. (A) and cell death (Annexin V staining) (B)

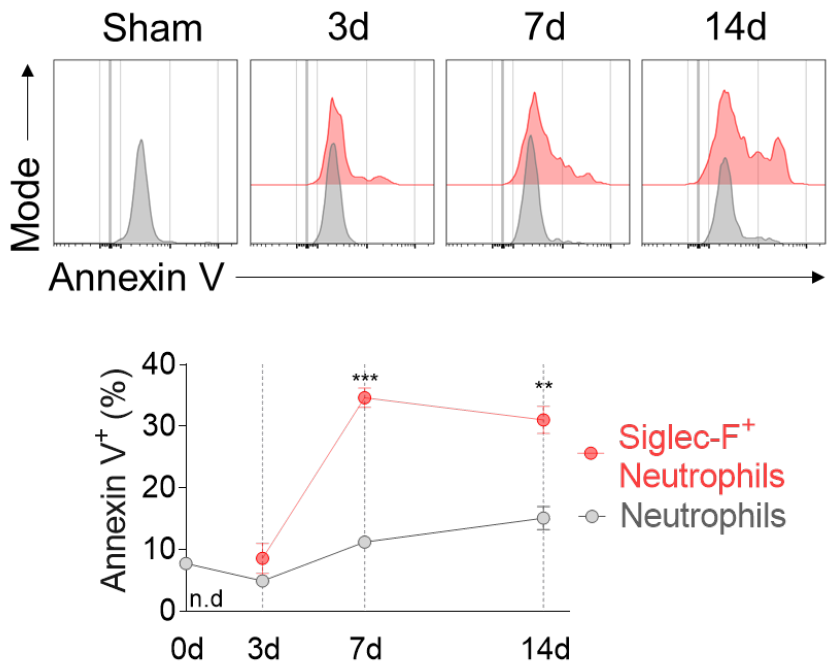


**Figure 23**. **Apoptosis of Siglec-F$^{+}$ neutrophils.**

Kinetic changes of the Siglec-F$^{+}$ and conventional neutrophil frequencies in terms of cell death (Annexin V staining). All results are shown as mean ± SEM and statistical analysis was performed using Mann-Whitney test. *P<0.05; ***P<0.001; n = 4-5 mice in each group. n.d.: not detected.

Then, I inquired as to the location of conventional neutrophils converting to Siglec-$F^+$ neutrophils. I knew it was not in the peripheral blood since blood lacked Siglec-$F^+$ neutrophils **(Figure 21)**. Thus, the conversions occurred either in the injured kidney's parenchyma or in the renal blood vessels. To ascertain which, mice treated with UUO were intravenously injected with a BV650-labeled CD45 monoclonal antibody (mAb) 5 minutes before to euthanasia, and the i.v. $CD45^+$ cells were examined **(Figure 24)**. This injection resulted in the formation of two distinct populations: BV650-$CD45^+$ leukocytes in the renal blood vessels and BV650-CD45- leukocytes in the parenchyma. As a control for this experiment, I evaluated the locations of neutrophils and macrophages in the renal parenchyma and vessels of CD45 mAb-injected naive animals. As expected, nearly all of the neutrophils in the kidneys of naive mice were circulating cells in the renal blood vessels, whereas half of the macrophages were found in the parenchyma of the kidney and half in the blood vessels **(Figure 25)**. On days 0, 3, 7, and 14 following the BV650-CD45 mAb injection, I evaluated the Siglec-$F^+$ neutrophils in the UUO-injured kidney. I discovered that the few Siglec-$F^+$ neutrophils present on day 0 and practically all in the renal arteries. By day 3 following UUO, half of the Siglec-$F^+$ neutrophils were found in the parenchyma, with the remaining half in the renal blood vessels. It was also observed on days 7 and 14 **(Figure 26)**. It is consistent with the hypothesis that UUO induces the conversion of conventional neutrophils in the renal blood arteries to Siglec-$F^+$ neutrophils, which then migrate into the renal parenchyma. Because these conversion events are ongoing, they both replace apoptotic Siglec-$F^+$ neutrophils and contribute to the expansion of the population over time.

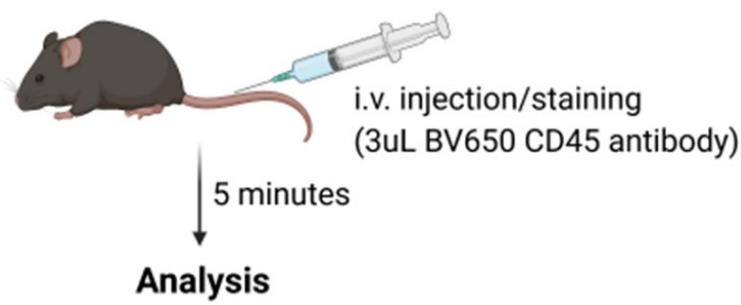


**Figure 24**. **Intravascular labeling of Siglec-F$^{+}$ neutrophils in the kidney.**

Sham- and UUO-treated mice were injected intravenously with a BV650-labeled CD45 mAb 5 minutes before they were euthanized. The figure was created with Biorender.com.

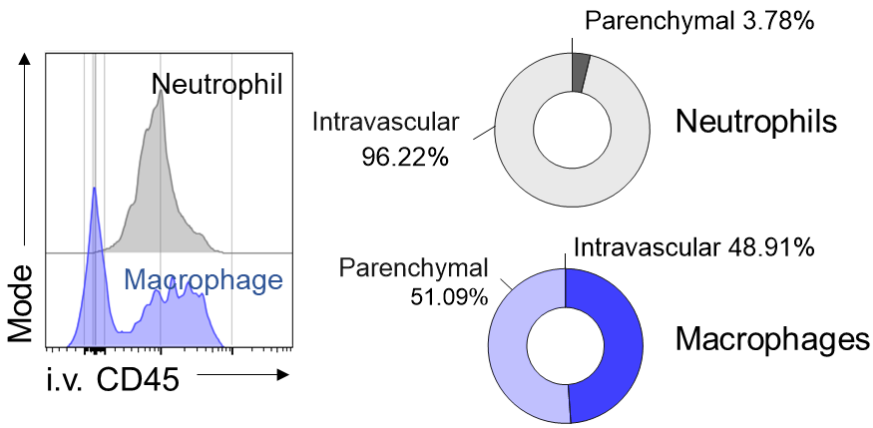


**Figure 25. Localization of neutrophils and macrophages in the homeostatic kidney.**

As a control to confirm that the mAb labeled the leukocytes in the kidney vasculature but not in the kidney parenchyma, naïve mice were injected with the BV650-CD45 mAb and the neutrophils and macrophages in the kidneys were subjected to flow cytometry. All results are shown as mean ± SEM. n = 4-5 mice in each group.

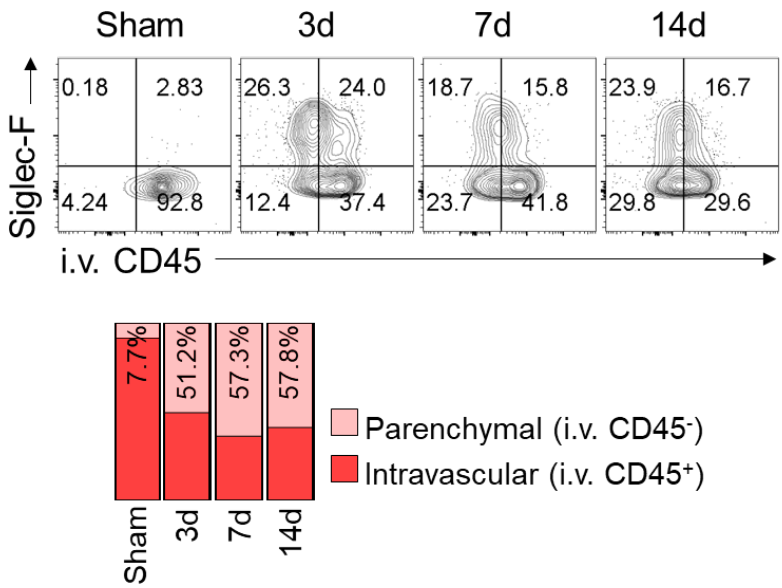


**Figure 26**. **Localization of Siglec-F$^{+}$ neutrophils in the kidney.**

(A) Sham- and UUO-treated mice were injected intravenously with a BV650-labeled CD45 mAb 5 minutes before they were euthanized. The BV650-CD45-labeled (intravascular, i.v.) and -unlabeled (parenchymal) Siglec-F$^{+}$ neutrophil frequencies in the UUO-damaged kidney over time were determined by flow cytometric analysis. All results are shown as mean ± SEM. n = 4-5 mice in each group.

## TGF-β1 and GM-CSF induce Siglec-F expression in neutrophils

To determine the factors that prompted conventional neutrophils to convert to Siglec-F$^{+}$ neutrophils following UUO, I evaluated the effect of UUO on the levels of known neutrophil plasticity-involving tissue cytokines[20, 43]. Thus, multiplex cytokine bead arrays were conducted using the kidney lysates of sham- and UUO-treated animals. TGF-β1, GM-CSF, IL-23, and monocyte chemoattractant protein-1 (MCP-1) were all immediately increased following UUO **(Figure 27)**. This was not the case with IL-1α, IFN-ɤ, TNF-α, IL-12p70, IL-6, IL-17A, IFN-β, IL-27, IL-10, or IL-1β **(Figure 28)**. Additionally, correlation analyses revealed that the levels of TGF-β1, GM-CSF, IL-23, and MCP-1 were significantly and positively correlated with the frequencies of Siglec-F$^{+}$ neutrophils **(Figure 29)**.

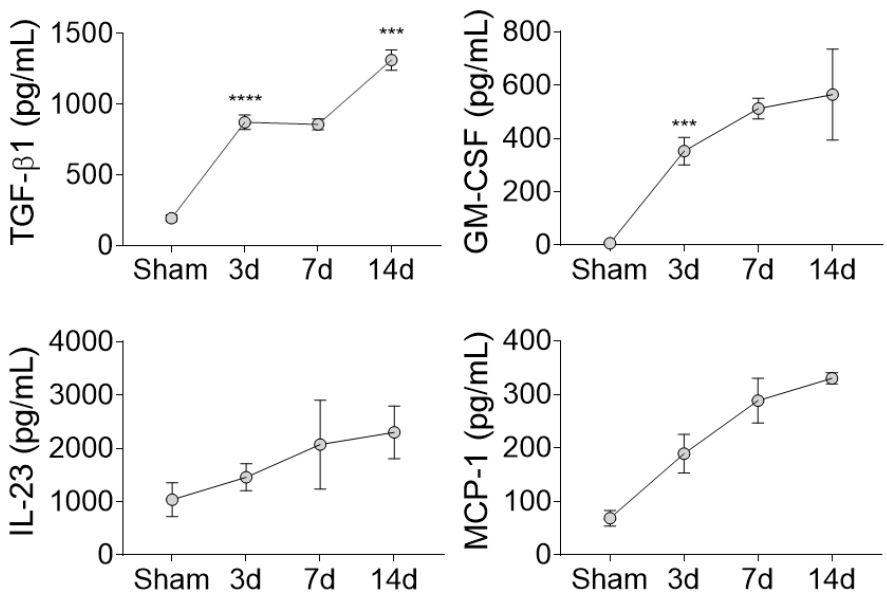


**Figure 27**. **Major tissue cytokine levels during UUO injury.**

Tissue cytokine levels increased in the UUO kidneys. All results are shown as mean ± SEM and statistical analysis was performed using one-way ANOVA test. *P<0.05; **P<0.01; ****P<0.0001; n = 4-5 mice in each group. (B) Correlation between the cytokines levels and frequency of Siglec-$F^+$ neutrophils in the kidney.

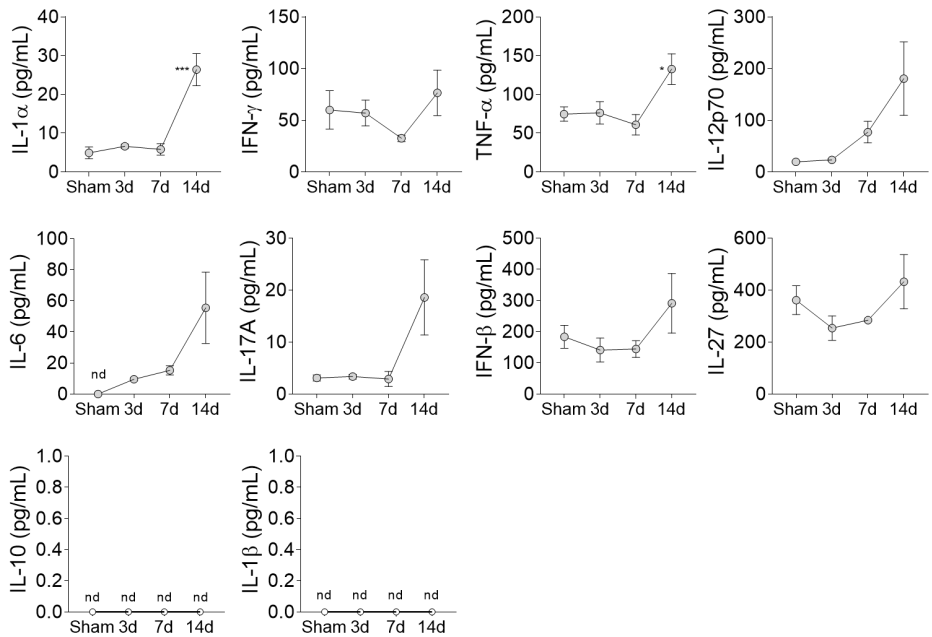


**Figure 28**. **Other tissue cytokine levels in the UUO injured kidneys.**

All results are shown as mean ± SEM and statistical analysis was performed using one-way ANOVA test. *P<0.05; ****P<0.0001; n = 4-5 mice in each group.

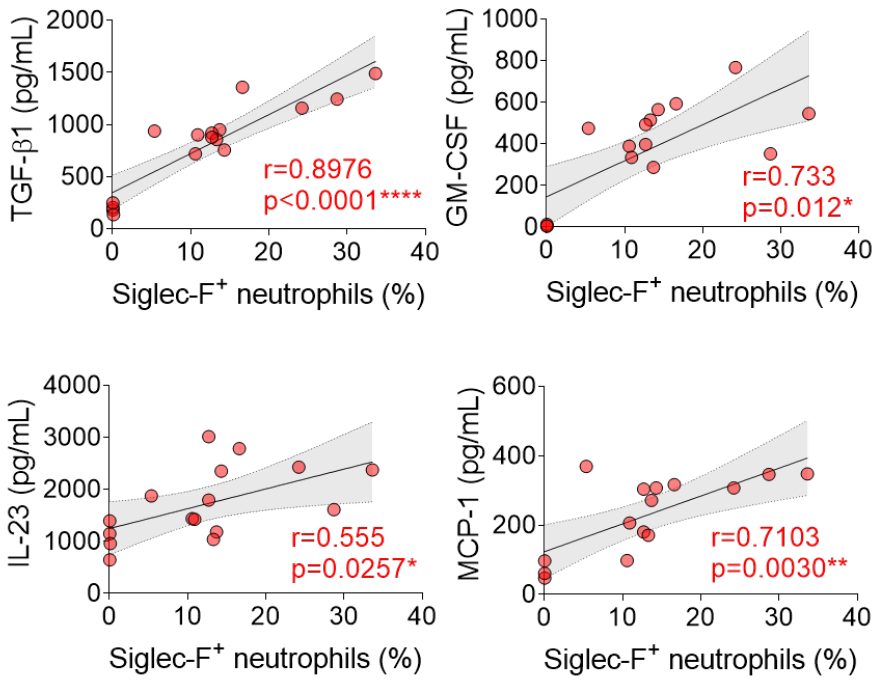


**Figure 29. Correlation between cytokine levels and the frequency of Siglec-F$^+$ neutrophils.**

Correlation between the cytokine levels and frequency of Siglec-F$^+$ neutrophils in the kidney. All results are shown as mean ± SEM and statistical analysis was performed using Pearson correlation analysis (B). *P<0.05; **P<0.01; ****P<0.0001; n = 4-5 mice in each group.

To examine whether TGF-β1, GM-CSF, IL-23, or MCP-1 directly trigger the conversion of conventional neutrophils to Siglec-F$^{+}$ neutrophils, I extracted neutrophils from murine bone marrow and treated them in vitro with each cytokine **(Figure 30)**. Siglec-F expression in neutrophils was induced by GM-CSF, but also by TGF-β1 (but not by IL-23 or MCP-1) **(Figure 31)**. Additionally, when TGF- β1 and GM-CSF were combined, they exhibited a minor additive effect on the number of Siglec-F$^{+}$ neutrophils in vitro **(Figure 31)**. To determine whether these cytokines acted similarly on human neutrophils, neutrophils were extracted from the peripheral blood of two healthy donors and treated with TGF-β1 and/or GM-CSF. Siglec-8 expression (the counterpart of mouse Siglec-F[44]) analysis revealed that GM-CSF (but not TGF-β1) increased Siglec-8$^{+}$ neutrophils, however there were discrepancies between donors **(Figure 32)**.

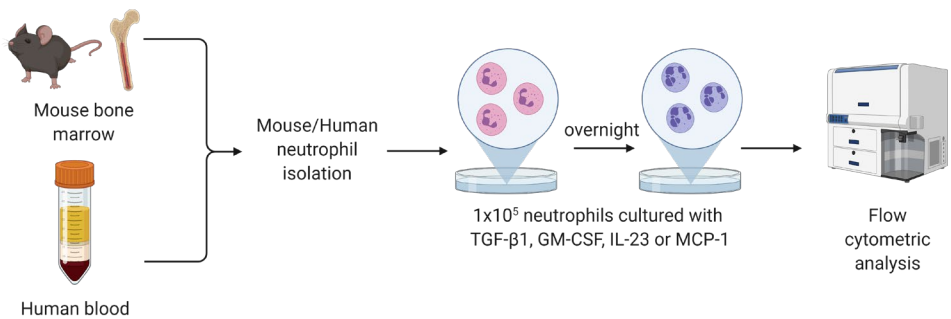


**Figure 30. Experimental scheme to convert the Siglec-F$^{+}$ or Siglec-8$^{+}$ neutrophils from cytokine stimulation.**

Neutrophils were harvested from mouse bone marrow or human blood, incubated overnight with 10 ng/ml of TGF-β1, GM-CSF, IL-23, and/or MCP-1, and then subjected to flow cytometric analysis of their Siglec-F (mouse) or Siglec-8 (human) expression. The figure was created with Biorender.com.

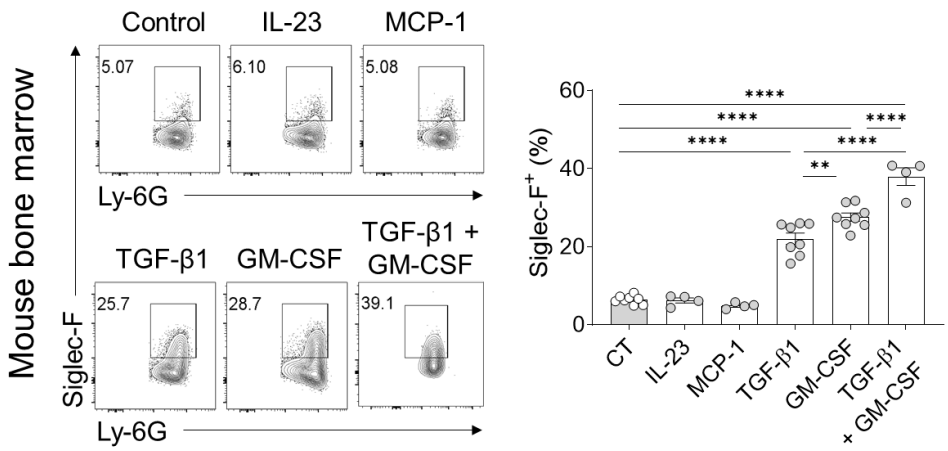


**Figure 31**. **In vitro conversion of mouse neutrophils to express Siglec-F.**

Mouse bone marrow derived neutrophils were incubated with 10ng/ml of each cytokine (or its combination) and analyzed for the expression of Siglec-F. All results are shown as mean ± SEM and statistical analysis was performed using one-way ANOVA test. **P<0.01; ****P<0.0001; n = 4-5 mice in each group.

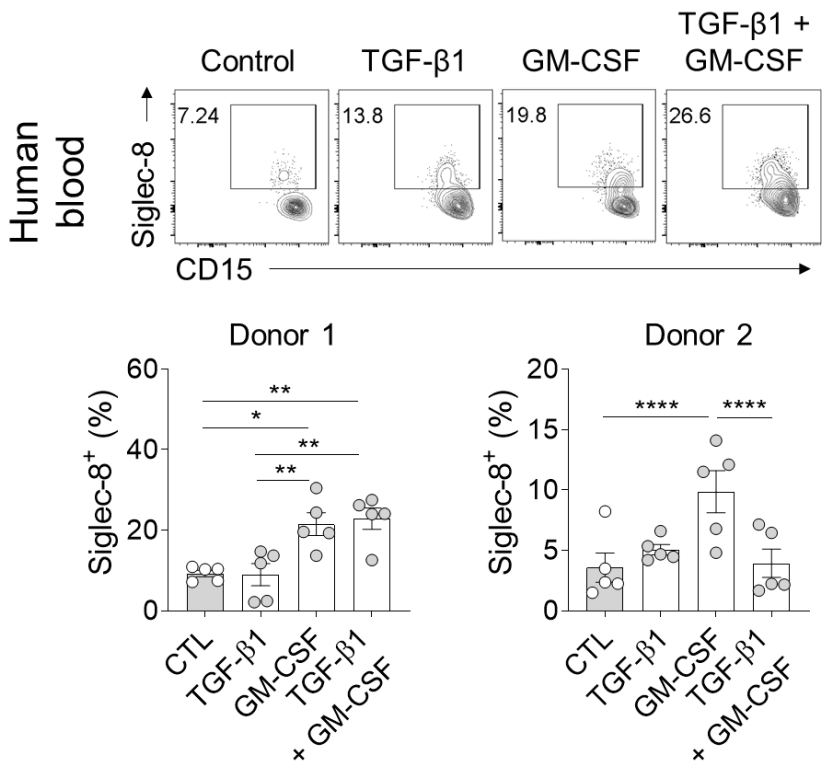


**Figure 32**. **In vitro conversion of human neutrophils to express Siglec-8.**

Human blood neutrophils were incubated with 10ng/ml of each cytokine (or its combination) and analyzed for the expression of Siglec-8. All results are shown as mean ± SEM and statistical analysis was performed using one-way ANOVA test. *P<0.05; **P<0.01; ****P<0.0001.

T cells are well-known producers of TGF-β1 and GM-CSF; they also play a critical role in the development of renal fibrosis[45, 46, 47]. I examined the immune cells of UUO kidneys in *Rag1*$^{-/-}$ mice (T and B cell-deficient mice) to establish whether T cells are the source of the TGF-β1 and GM-CSF that lead conventional neutrophils to change to Siglec-F$^{+}$ neutrophil. Siglec-F$^{+}$ neutrophils were detected in *Rag1*$^{-/-}$ mice, but at a lower frequency than in WT animals (5% vs. 25% of CD45$^{+}$ cells) **(Figure 33)**. Thus, while T cells contribute some of these cytokines, it is likely that non-immune cells such as tubular epithelial cells (which have been shown to produce TGF-β1 and GM-CSF during renal fibrosis[48, 49]) also contribute to the induction of Siglec-F$^{+}$ neutrophils through the production of pro-inflammatory cytokines.

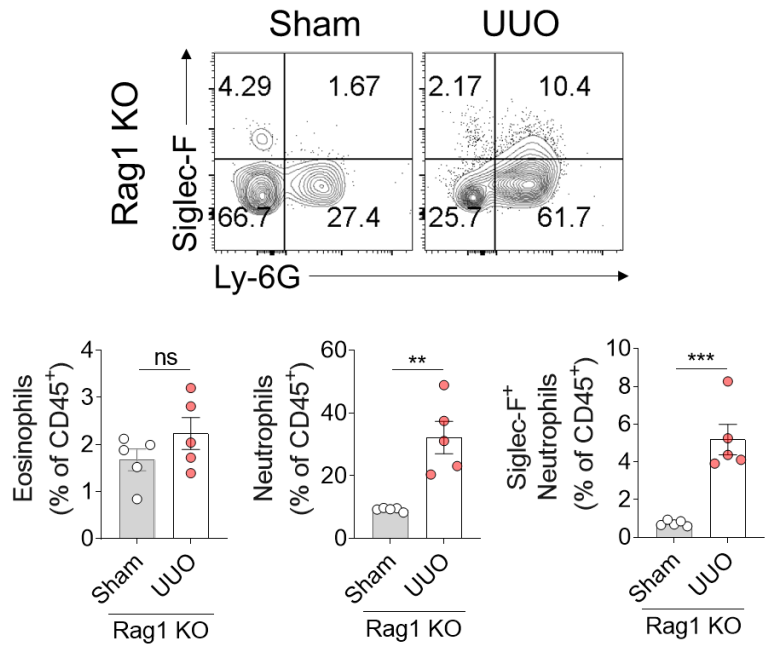


**Figure 33**. **UUO injury models in Rag1 knockout mice.**

All results are shown as mean ± SEM and statistical analysis was performed using Student's t-test. ***P*<0.01; ****P*<0.001; n = 5 mice in each group. ns, not significant.

## Siglec-F$^+$ neutrophils produce pro-fibrotic factors that activate fibroblasts and Collagen 1

As previously stated, Siglec-F$^+$ neutrophils were more likely than conventional neutrophils to exhibit hyper-segmentation in the kidney following UUO **(Figure 15)**. Given that neutrophil hyper-segmentation is associated with a unique proteome and function[50], I evaluated the expression of inflammatory and homeostatic markers[50, 51] on conventional and Siglec-F$^+$ neutrophils in the kidney following UUO. Siglec-F$^+$ neutrophils showed significantly higher expression of CD11b and leucine-rich repeat-containing protein 32 (LRRC32), but CD62L expression was significantly lower. LRRC32 activates the latent form of TGF-β1[52]. However, there was no difference in the surface levels of Dectin-1 between the two neutrophil populations, which is an inflammatory mediator increased in polarized neutrophils[51] **(Figure 34)**. Intracellular cytokine staining revealed that Siglec-F$^+$ neutrophils from the UUO-injured kidney expressed much more TGF-β1, TNF-α, and IL-1β than conventional neutrophils **(Figure 35)**. Quantitative PCR study of sorted neutrophils from UUO-injured kidneys verified this result **(Figure 36)**.

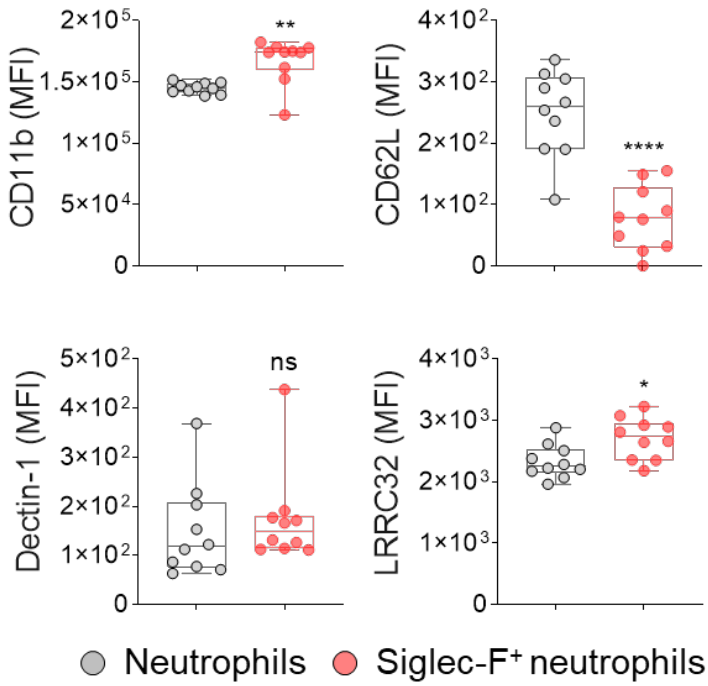


**Figure 34. Activated features of Siglec-F$^+$ neutrophils.**

Flow cytometric comparison of conventional neutrophils and Siglec-F$^+$ neutrophils in the UUO-injured kidney at day 7 (n = 10 in each group) in terms of their surface levels of inflammatory and homeostatic markers. All results are shown as mean ± SEM and statistical analysis was performed using Student's t-test. *P<0.05; **P<0.01; ****P<0.0001; ns, not significant; MFI, mean fluorescence intensity.

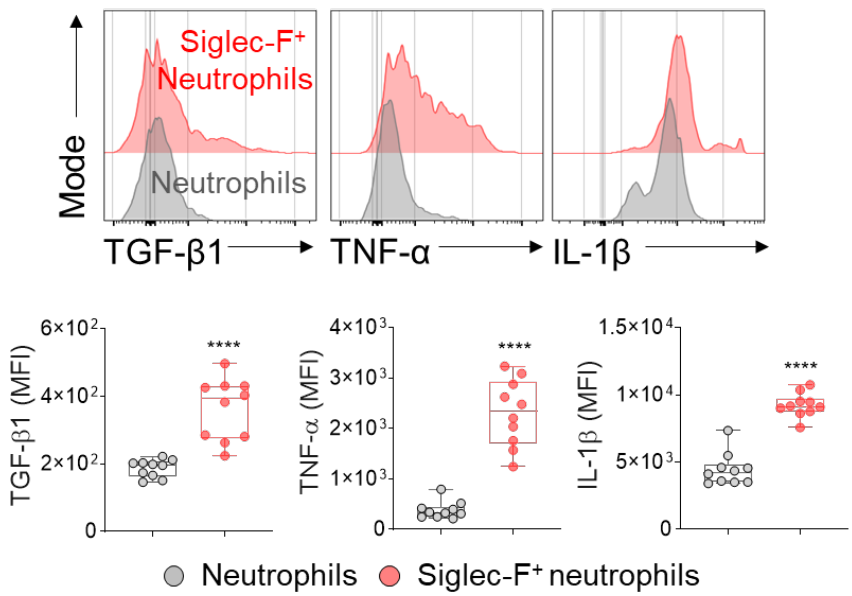


**Figure 35. Flow cytometric analysis of proinflammatory cytokines expressed by Siglec-F$^+$ neutrophils.**

Flow cytometric comparison of conventional neutrophils and Siglec-F$^+$ neutrophils in the UUO-injured kidney at day 7 (n = 10 in each group) in terms of expression of pro-fibrotic and pro-inflammatory cytokines. All results are shown as mean ± SEM and statistical analysis was performed using Student's t-test. *P<0.05; **P<0.01; ****P<0.0001; ns, not significant; MFI, mean fluorescence intensity.

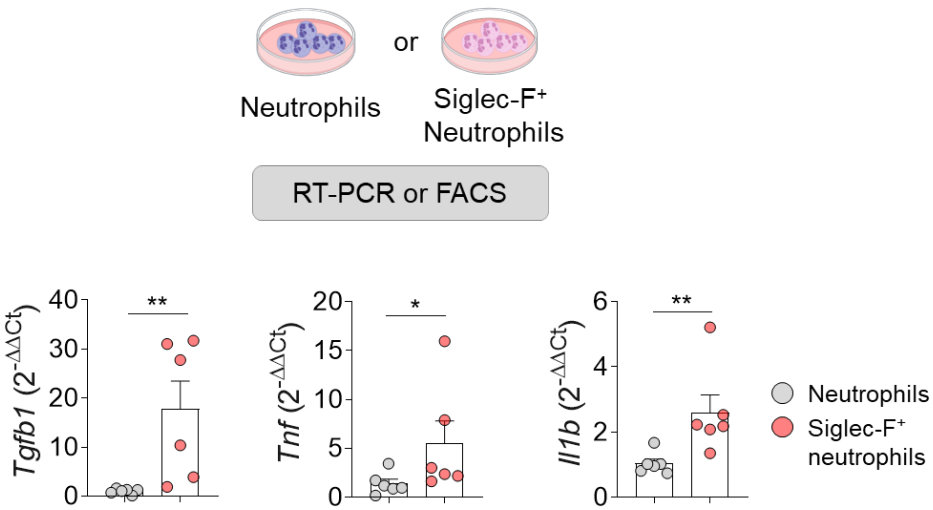


**Figure 36**. **qPCR analysis of proinflammatory cytokines expressed by Siglec-F$^+$ neutrophils.**

RT-qPCR analysis of sorted neutrophils and Siglec-F$^+$ neutrophils from UUO-induced kidney (n = 6 in each group). All results are shown as mean ± SEM and statistical analysis was performed using Mann-Whitney test. *$P$<0.05; **$P$<0.01. The figure was created with icons from Biorender.com.

Our in vitro work demonstrated that TGF-β1 and, more specifically, GM-CSF converted neutrophils from murine bone marrow into Siglec-$F^+$ neutrophils **(Figure 31)**. When examined the levels of pro-inflammatory cytokines produced by Siglec-$F^+$ neutrophils again with RT-PCR, I confirmed that treatment with GM-CSF, but not TGF-β1, prompted these cells to express the pro-inflammatory genes TGF-β1 and TNF-α **(Figure 37)**. Given that TGF-β1, TNF-α, and IL-1β are known to trigger fibrotic activity of fibroblasts[53, 54], these findings prompted us to speculate that pro-inflammatory cytokines produced by Siglec-$F^+$ neutrophils cause fibroblast activation and differentiation. To examine this, I co-cultured in vitro unprimed (conventional) neutrophils with NIH3T3, a mouse embryonic fibroblast cell line, or with TGF-β1 or GM-CSF-primed neutrophils. I rinsed away the neutrophils after 24 hours and analyzed the fibroblasts using Western blot analysis for two fibroblast activation and differentiation markers, COL1A1 and α-SMA **(Figure 38)**. Both were increased in fibroblasts cultured with primed neutrophils. Additionally, consistent with GM-CSF effect on Siglec-F expression of neutrophils **(Figure 31)**, GM-CSF-primed neutrophils activated fibroblasts more potently than TGF-β1-primed neutrophils **(Figure 39)**.

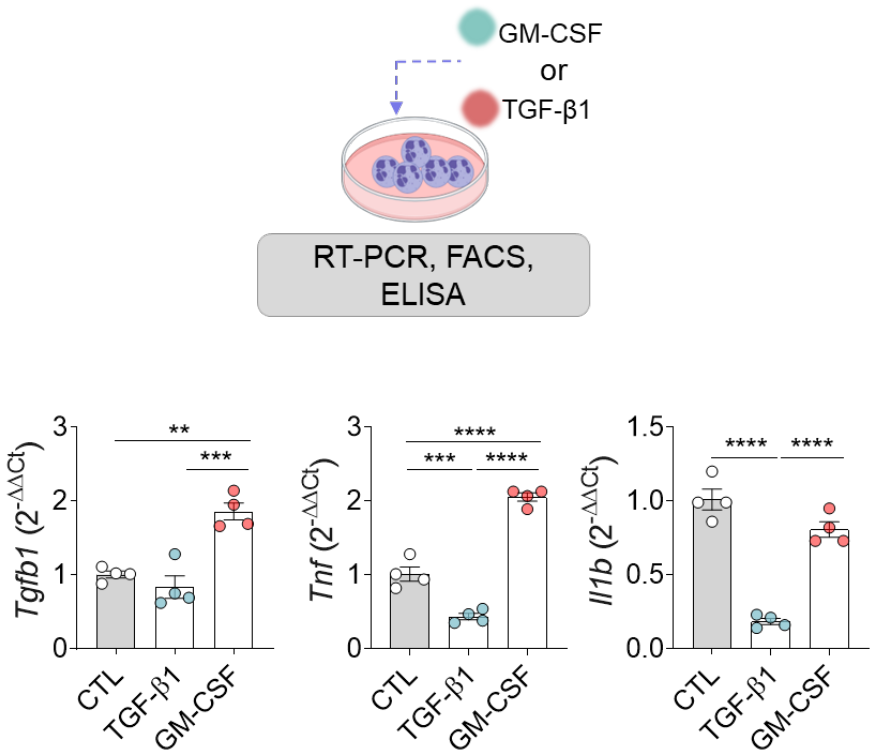


**Figure 37. Proinflammatory cytokines expressed by in vitro generated Siglec-F$^{+}$ neutrophils.**

RT-qPCR analysis of TGF-β1 or GM-CSF primed neutrophils (n = 4 in each group). All results are shown as mean ± SEM and statistical analysis was performed using one-way ANOVA test. **P<0.01; ***P<0.001; ****P<0.0001. The figure was created with icons from Biorender.com.

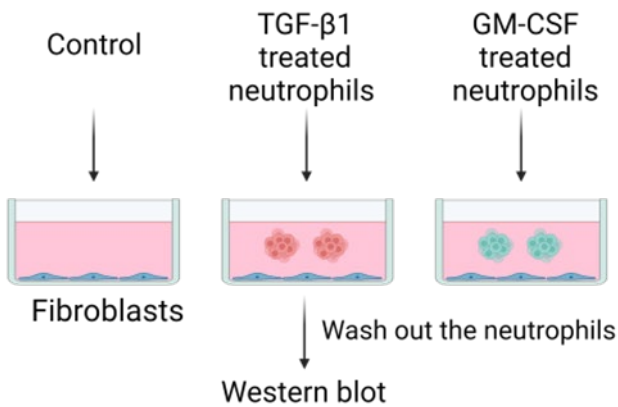


**Figure 38**. **Co-culture system of fibroblasts and primed neutrophils.**

Depiction of the experiment (n = 6 in each group) where bone marrow-derived neutrophils were induced to convert into Siglec-$F^{+}$ neutrophils by priming with TGF-β1 or GM-CSF, after which they were co-cultured with NIH3T3 fibroblasts. The figure was created with Biorender.com

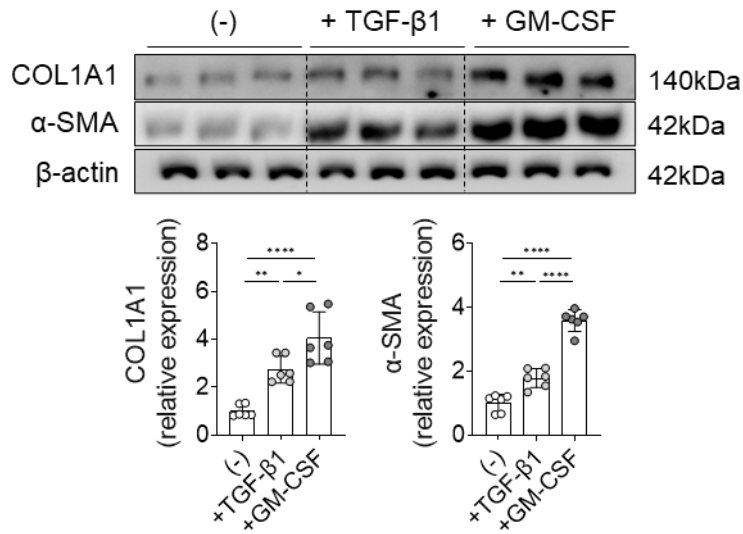


**Figure 39**. **Activation of fibroblasts by culturing with primed neutrophils.**

Western blot analysis for COL1A1 and α-SMA, which are fibroblast activation and differentiation markers. All results are shown as mean ± SEM and statistical analysis was performed using one-way ANOVA test. *P<0.05; **P<0.01; ****P<0.0001.

Recent research has demonstrated that fibroblasts are not the only cells capable of producing Collagen 1 in renal fibrosis; immune cells, notably macrophages, also possess this capability[55, 56]. Indeed, when I used flow cytometry to compare COL1A1-expressing $CD45^+$ immune cells and $CD45^-$ non-immune cells in sham- and UUO-treated kidneys, I discovered that UUO significantly increased the number of COL1A1-producing $CD45^+$ immune cells (from 4 percent in the sham-treated mice to 70 percent in the UUO-treated mice). After UUO, a study of immune cell types revealed that the great majority of $CD45^+$ leukocytes expressing COL1A1 were Siglec-$F^+$ neutrophils **(Figure 40)**. I then validated by immunofluorescence staining and quantitative RT-PCR that Siglec-$F^+$ neutrophils isolated from UUO kidneys expressed COL1A1; conventional neutrophils, on the other hand, did not express COL1A1 **(Figures 41A and 41B)**. Similarly, bone marrow-derived neutrophils stimulated in vitro with GM-CSF expressed much more COL1A1 than unprimed neutrophils **(Figure 42A and 42B)**. Overall, Siglec-$F^+$ neutrophils contribute to renal fibrosis in two ways: by activating fibroblasts via pro-fibrotic cytokines (TGF-β1, TNF-α, and IL-1β), and by secreting COL1A1 directly.

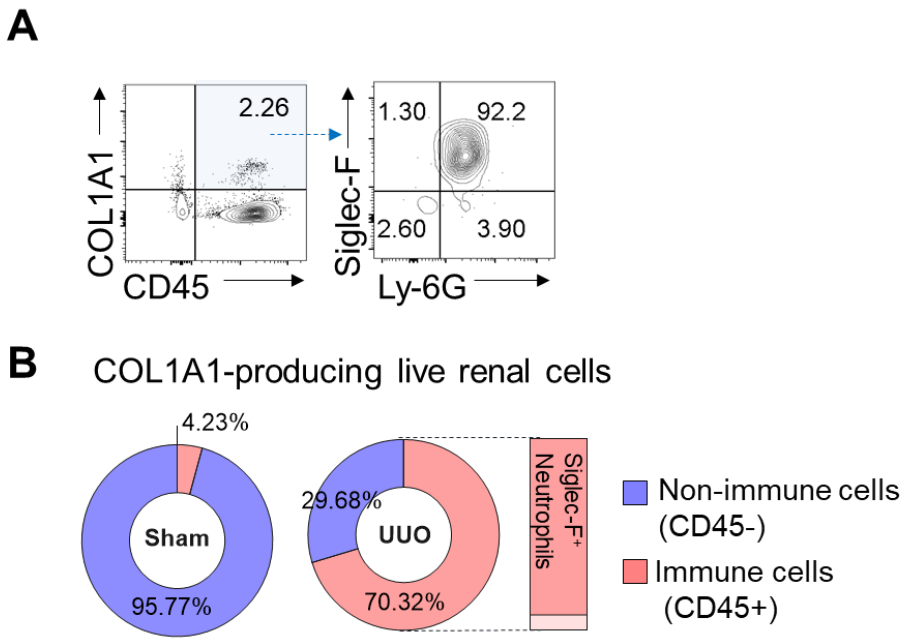


**Figure 40. Flow cytometric analysis of collagen 1 expression in Siglec-F$^+$ neutrophils from UUO kidney.**

Flow cytometric analysis of the intracellular levels of COL1A1 in the CD45$^+$ immune cells and CD45$^-$ non-immune cells from sham- and UUO-treated kidneys at day 7. (A) Flow cytometric analysis of UUO kidney. (B) Pie chart showing the frequency of COL1A1 producing Siglec-F$^+$ neutrophils.

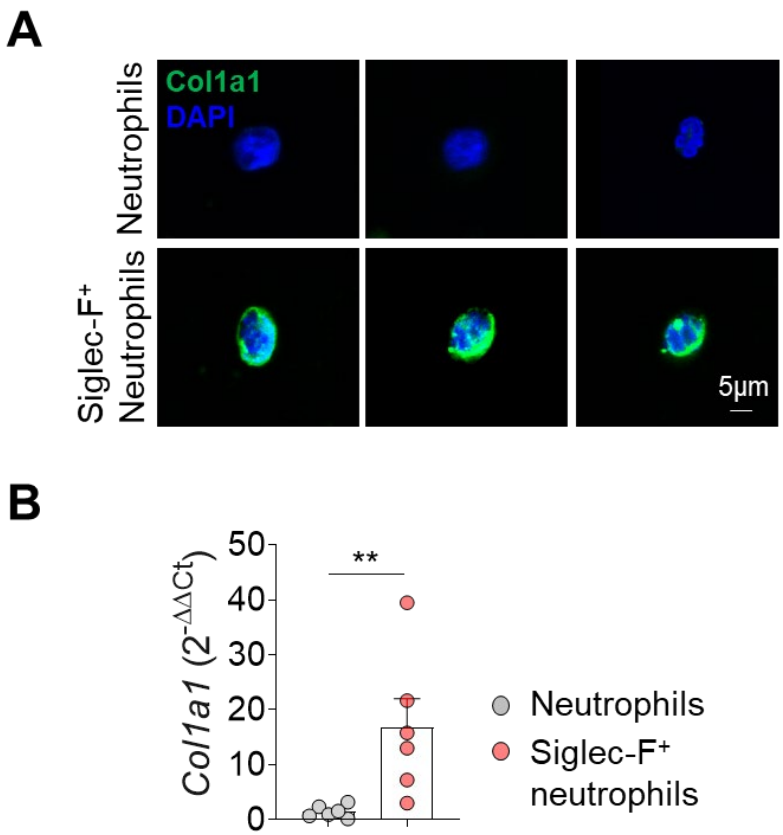


**Figure 41**. **Collagen 1 expression in the sorted Siglec-F$^+$ neutrophils from UUO kidney.**

Sorted conventional and Siglec-F$^+$ neutrophils from UUO-treated kidneys at day 14 (n = 6 in each group) were subjected to immunofluorescence (A) and RT-qPCR (B) analysis of COL1A1 protein expression. All results are shown as mean ± SEM and statistical analysis was performed using Student's t-test. **P<0.01.

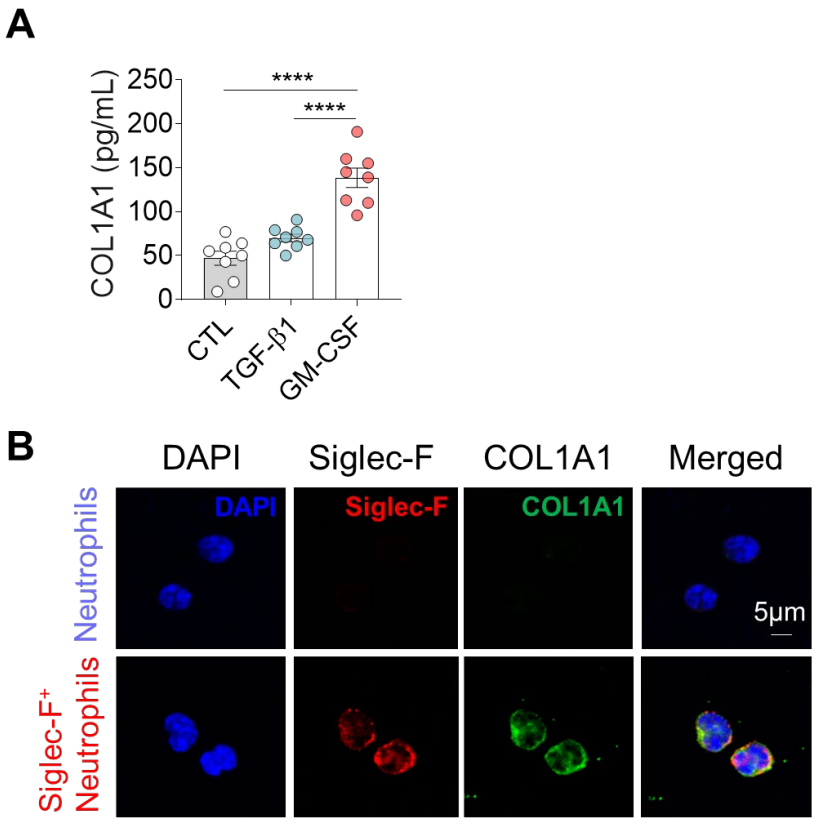


**Figure 42. Collagen 1 expression in Siglec-F$^{+}$ neutrophils generated in vitro.**

COL1A1 expression of TGF-β1 or GM-CSF primed neutrophils evaluated by ELISA (n = 8 in each group) (A) and immunofluorescence (B). All results are shown as mean ± SEM and statistical analysis was performed using one-way ANOVA test (B-C). ****$P$<0.0001.

## Siglec-F$^+$ neutrophils contribute to the advanced renal fibrosis

To determine whether Siglec-F$^+$ neutrophils are required for renal fibrosis, I depleted Siglec-F$^+$ neutrophils on days 2 and 4 following UUO using anti-Siglec-F or anti-Ly-6G antibodies **(Figure 43A)**. On day 7, flow cytometry revealed that anti-Ly-6G antibodies decreased both Siglec-F$^+$ and conventional neutrophils in the kidney, but anti-Siglec-F antibodies depleted only Siglec-F$^+$ neutrophils **(Figure 43B)**. Fibrosis in the kidneys was assessed using Sirius red histology and COL1A1 immunohistochemistry. While both antibodies were successful at reducing fibrosis, the anti-Siglec-F antibody was significantly more effective **(Figure 44)**. Additionally, it inhibited the expression of renal injury and fibrosis-related markers in the kidney more effectively than the anti-Ly-6G antibody **(Figure 45)**. Above all, it meant that the contribution of conventional neutrophils in inducing renal fibrosis was minimal. This discrepancy may be explained in part by the significant rise in Siglec-F$^+$ CCR3$^+$ eosinophils in anti-Ly-6G-treated UUO mice (25.8% vs. 4.3% in isotype-treated mice and 0.9% in anti-Siglec-F-treated mice) **(Figure 43B)**, which may cause fibrosis. Consistent with these findings, the frequency of Siglec-F$^+$ neutrophils was extremely significant and positively correlated with the degree of renal fibrosis as determined by Sirius red and COL1A1 staining **(Figure 46)**.

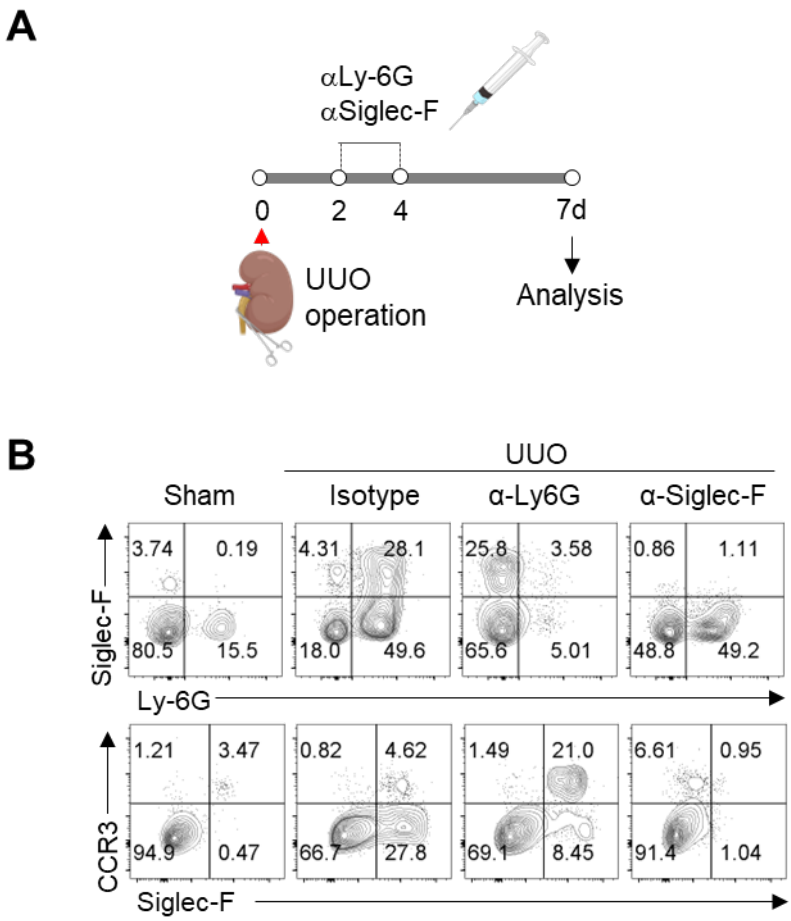


**Figure 43. Experimental of Siglec-F$^+$ neutrophil depletion in UUO mice.**

(A) UUO mice were treated on days 2 and 4 with isotype control, anti-Ly-6G, or anti-Siglec-F mAbs. The figure was created with icons from Biorender.com. (B) The anti-Ly-6G and anti-Siglec-F mAbs effectively depleted the Siglec-F$^+$ neutrophils in the kidney; the anti-Ly-6G antibodies also depleted the conventional neutrophils in the kidney.

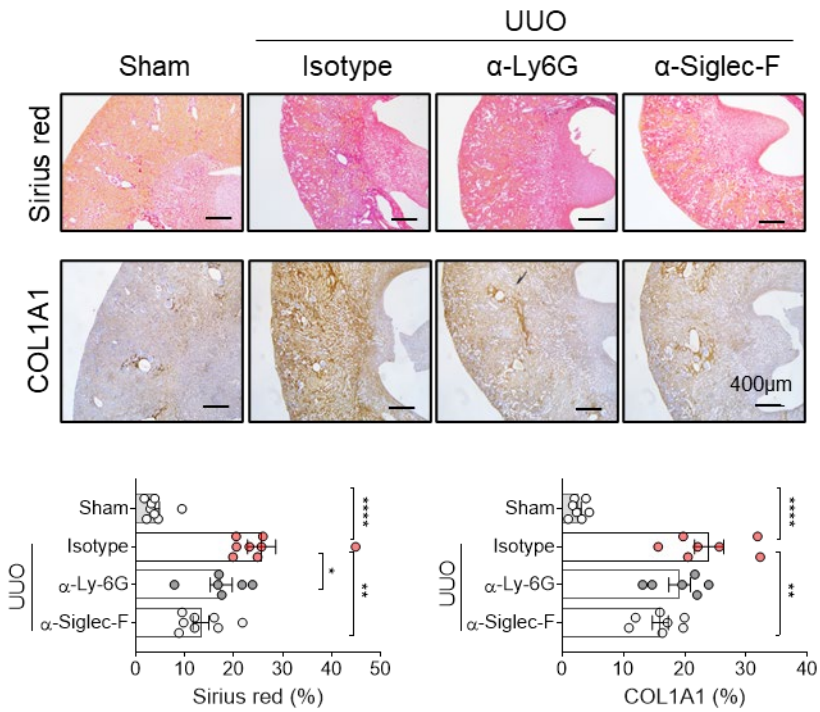


**Figure 44**. **Histologic analysis of Siglec-F$^{+}$ neutrophil depletion in UUO mice.**

The effect of Siglec-F$^{+}$ neutrophil depletion on the renal fibrosis was determined on day 7 by Sirius-red histology and COL1A1 immunohistochemistry. All results are shown as mean ± SEM and statistical analysis was performed using one-way ANOVA test. **P*<0.05; ***P*<0.01; *****P*<0.0001; n = 6-7 mice in each group.

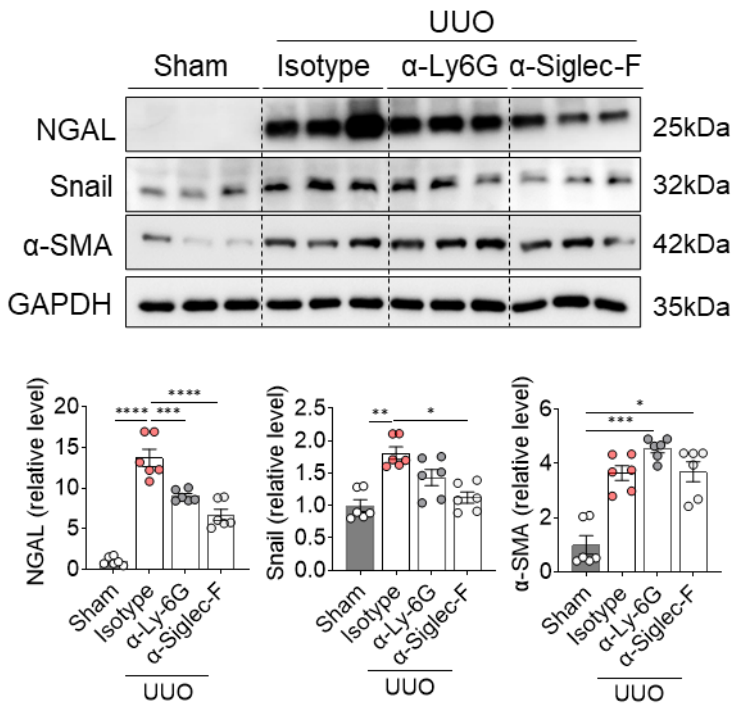


**Figure 45**. **Western blot analysis of Siglec-F$^{+}$ neutrophil depletion in UUO mice.** The effect of Siglec-F$^{+}$ neutrophil depletion on the degree of renal injury was determined on day 7 by Western blotting of kidney damage- and fibrosis-related markers. All results are shown as mean ± SEM and statistical analysis was performed using one-way ANOVA test. **P*<0.05; ***P*<0.01; ****P*<0.001; *****P*<0.0001; n = 6-7 mice in each group.

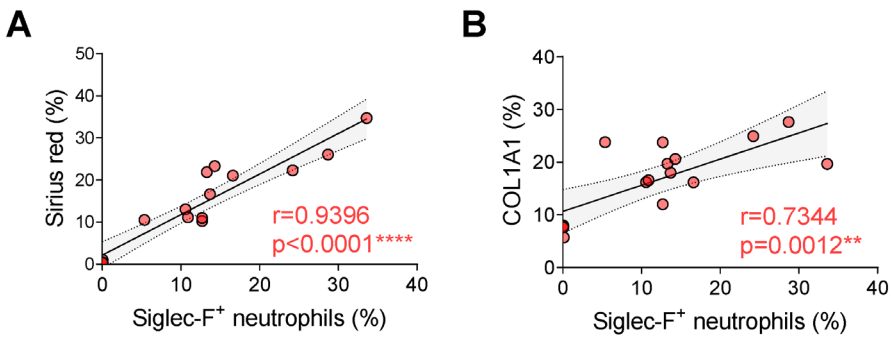


**Figure 46. Correlation between Siglec-F$^{+}$ neutrophils and fibrosis markers.**

Pearson correlation analysis between Siglec-F$^{+}$ neutrophil frequencies and the percentage of Sirius red- and COL1A1-staining in the UUO-damaged kidneys. ***P*<0.01; *****P*<0.0001.

To investigate whether Siglec-F$^{+}$ neutrophils directly produce renal fibrosis, I adoptively transplanted Siglec-F$^{+}$ neutrophils made in vitro into control and UUO mice **(Figure 47)**. Renal fibrosis was dramatically increased in UUO mice when Siglec-F$^{+}$ neutrophils were intravenously delivered to the kidney; however, adoptive transfer of Siglec-F$^{+}$ neutrophils into control mice had no effect on renal fibrosis **(Figures 48A and B)**. Indeed, transferred Siglec-F$^{+}$ neutrophils were barely detected in control mouse kidneys, indicating that i.v. transferred Siglec-F$^{+}$ neutrophils did not migrate to the uninjured kidney **(Figure 49)**.

Taken together, these findings support the hypothesis that Siglec-F$^{+}$ neutrophils are critical in the development of renal fibrosis.

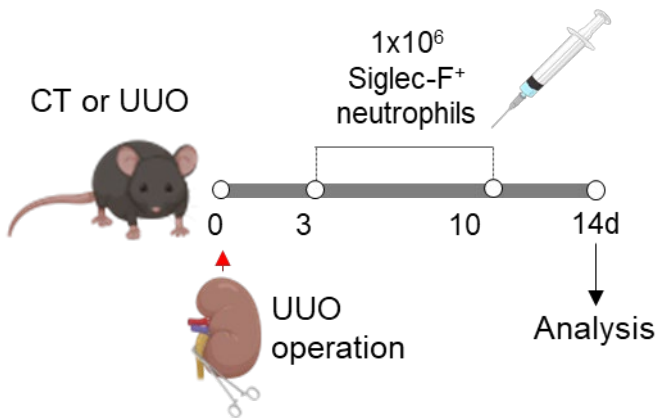


**Figure 47. Experimental scheme of adoptive transfer of Siglec-F$^+$ neutrophils in healthy and UUO mice.**

(A) Experimental scheme. Siglec-F$^+$ neutrophils were adoptively transferred into the control or UUO mice on days 3 or 10 from the injury. The figure was created with icons from Biorender.com.

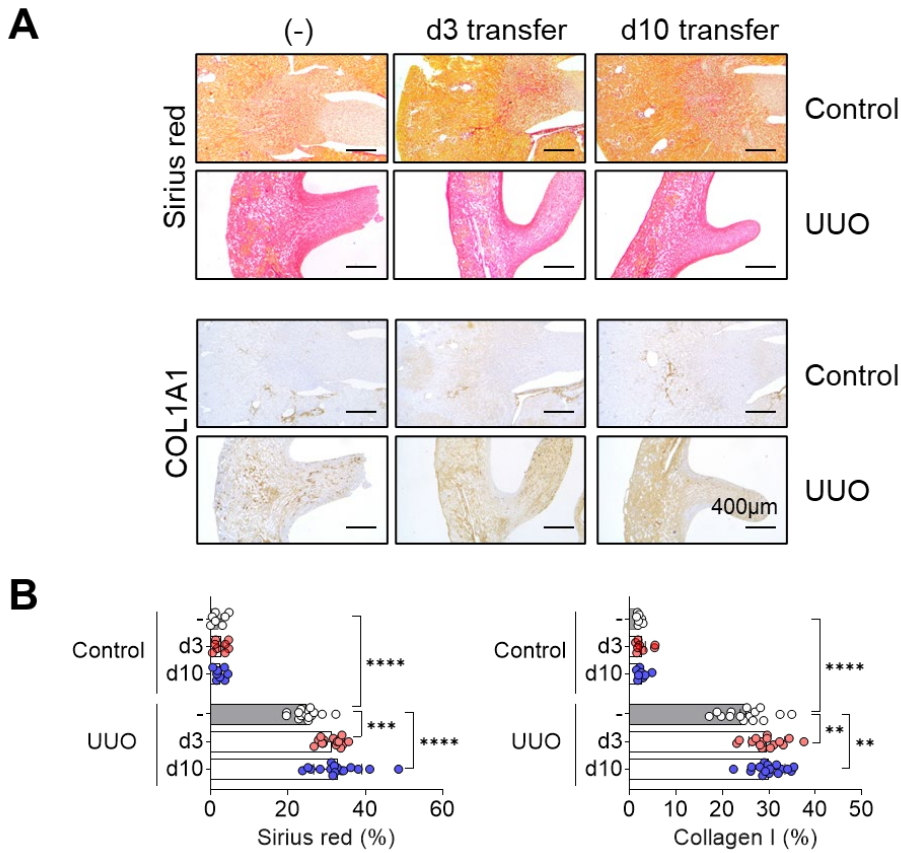


**Figure 48. Histological analysis of adoptive transfer of Siglec-F$^+$ neutrophils in healthy and UUO mice.**

Siglec-F$^+$ neutrophils were adoptively transferred into the control or UUO mice on days 3 or 10 from the injury. (A-B) The effect of adoptive transfer of Siglec-F$^+$ neutrophils on the degree of renal injury was determined on day 14 by Sirius-red histology and COL1A1 immunohistochemistry. All results are shown as mean ± SEM and statistical analysis was performed using one-way ANOVA test. **P<0.01; ***P<0.001; ****P<0.0001; n=7-16 mice in each group.

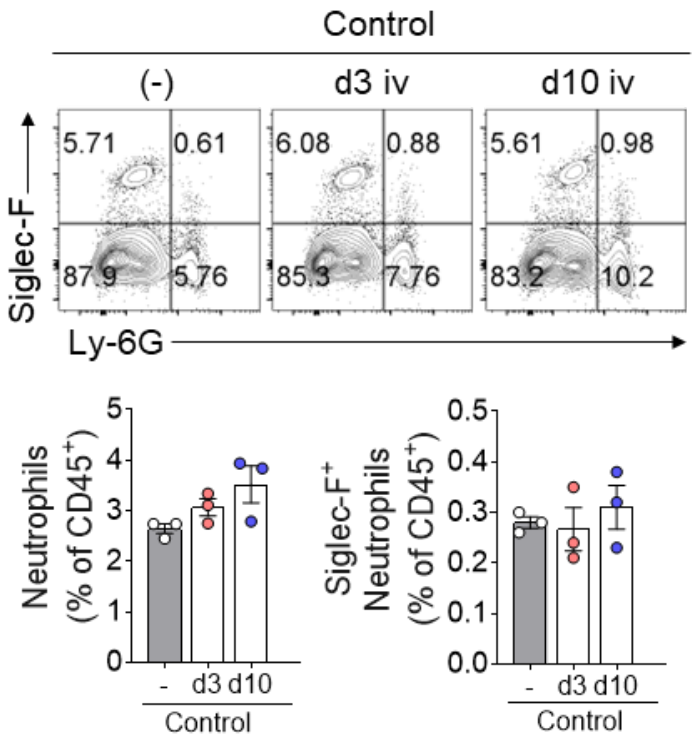


**Figure 49**. **Adoptive transfer of Siglec-F$^+$ neutrophils to control mice.**

Conventional and Siglec-F$^+$ neutrophils in Siglec-F$^+$ neutrophil transferred control mouse kidneys. All results are shown as mean ± SEM and statistical analysis was performed using one-way ANOVA test. n=3 mice in each group.

## Siglec-F$^+$ neutrophils are increased in the kidneys of other murine CKD models and human kidneys with renal cell carcinoma

Finally, I examined whether Siglec-F$^+$ neutrophils are similarly involved in the advancement of fibrosis in CKD models induced by various other etiologies. Adriamycin-induced nephropathy serves as a model for focal segmental glomerulosclerosis (FSGS) and has the benefit of inducing glomerular and tubular interstitial fibrosis[57]. Likewise, the UUO model, Adriamycin-induced nephropathy is accompanied with an increase in Siglec-F$^+$ neutrophils in the kidney **(Figure 50)**. Because UUO and Adriamycin nephropathy are both models of acute renal fibrosis, I also studied the renal ischemia-reperfusion injury (IRI) model, which has the advantage of modeling the transitions from acute kidney injury to CKD[58] **(Figure 51A)**. Fibrosis developed slowly in the IRI model, as expected. However, 4 and 8 weeks following the kidney damage, a considerable rise in Siglec-F$^+$ neutrophil frequencies was detected **(Figure 51B)**. Thus, Siglec-F$^+$ neutrophils may have a role in a variety of fibrotic renal disorders.

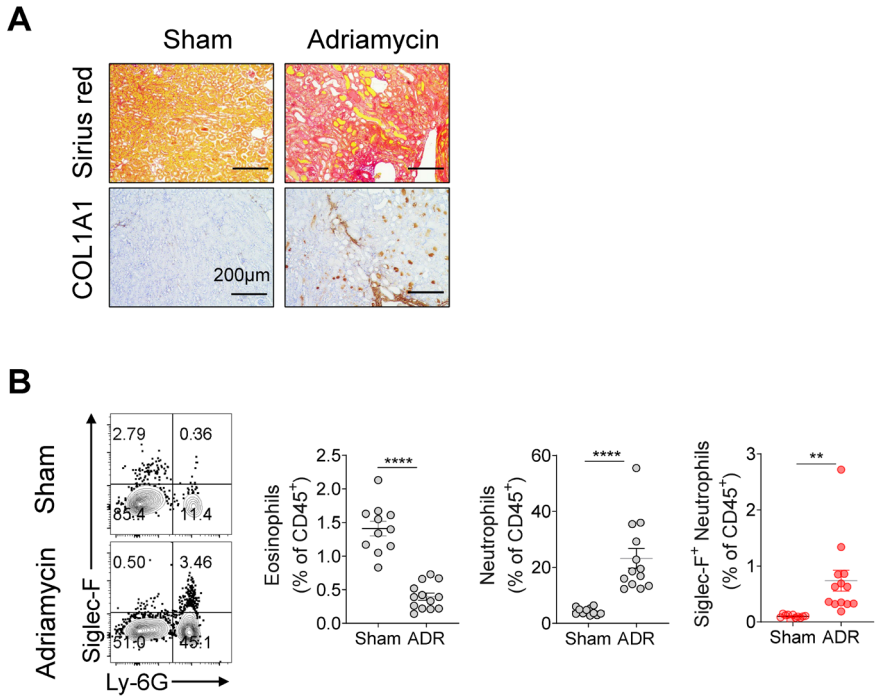


**Figure 50**. **Adriamycin induced nephropathy.**

Adriamycin-induced nephropathy was induced and evaluated on day 7. (A) The induction of fibrosis was measured by Sirius red histology and COL1A1 immunohistochemistry**.** (B) The changes in eosinophil, neutrophil, and Siglec-F$^{+}$ neutrophil frequencies were determined by flow cytometry. All results are shown as mean ± SEM and statistical analysis was performed using Student's t-test. ***P*<0.01; *****P*<0.0001. n = 11-13 mice in each group.

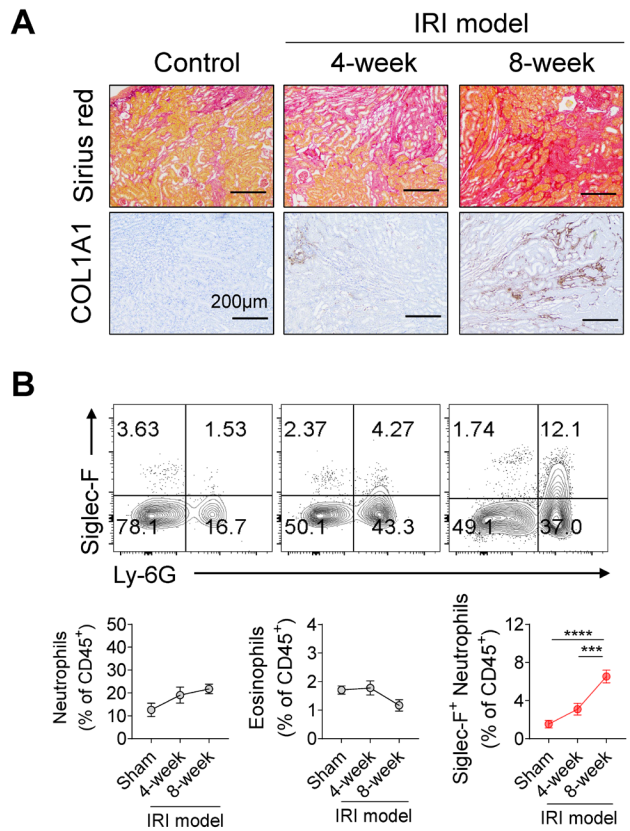


**Figure 51**. **Renal ischemia-reperfusion injury model.**

Renal ischemia-reperfusion injury (IRI) was induced and evaluated on week 4 and 8. (A) The induction of fibrosis was measured by Sirius red histology and COL1A1 immunohistochemistry**.** (B) The changes in eosinophil, neutrophil, and Siglec-$F^+$ neutrophil frequencies were determined by flow cytometry. All results are shown as mean ± SEM and statistical analysis was performed using one-way ANOVA test. ***$P$<0.001; ****$P$<0.0001. n = 8 mice in each group.

To extend our findings from mice CKD models to human renal fibrosis, I investigated a publicly available database of gene expression from CKD patients (Nephroseq Research Edition. Ann Arbor, MI: University of Michigan; http://www.nephroseq.org). Because humans lack the Siglec-F gene, I instead studied Siglec-8, which is a mouse Siglec-F paralog. In comparison to healthy renal tissues, the renal tissues of individuals with diabetic nephropathy (DN) and FSGS expressed considerably more *FCGRIIIB* (a neutrophil surrogate marker) and *SIGLEC8* **(Figure 52A)**. Additionally, the expression of both genes was strongly and negatively linked with the renal function of DN patients, namely the log2 glomerular filtration rate (GFR) **(Figure 52B)**. These findings imply that Siglec-$8^+$ neutrophils are increased in patients with CKD and may be associated with disease aggravation.

Because intratumoral fibrosis is a frequent characteristic of clear cell renal cell carcinoma (RCC)[59], I also examined the Siglec-$8^+$ neutrophils in the renal tissues of seven RCC patients. Indeed, I confirmed that tumor tissues in surgical specimens had a higher level of fibrosis and collagen deposition than normal kidney tissues **(Figure 53)**. When healthy and tumor kidney tissues from the same donor were compared, Siglec-$8^+$ neutrophils were found solely in the tumor fractions **(Figure 54)**. Together, these findings support the concept that this novel neutrophil subpopulation contributes to renal fibrosis in both murine and human kidneys.

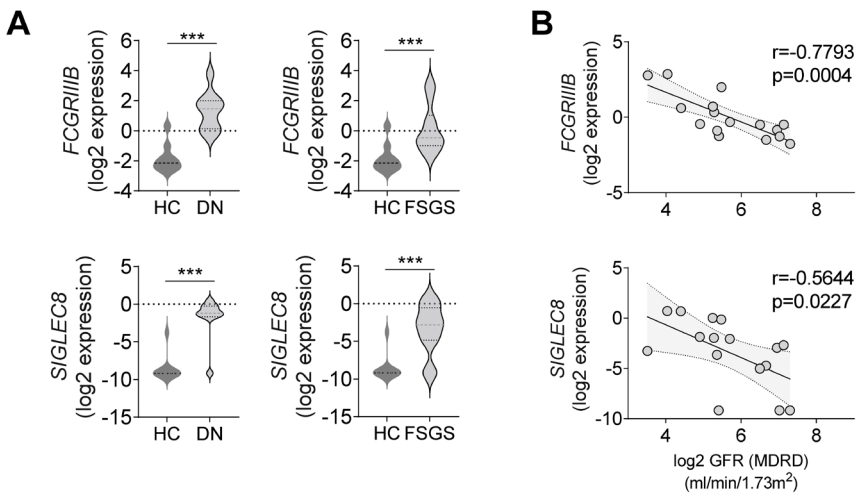


**Figure 52**. **Expression of *SIGLEC8* and *FCGRIIIB* in the CKD patients.**

A public gene expression dataset of CKD patients was used to determine whether diabetic nephropathy (DN) (n = 9) and focal segmental glomerulosclerosis (FSGS) (n = 19) associated with increased renal frequencies of neutrophils (as indicated by the *FCGRIIIB* gene) and Siglec-8$^{+}$ neutrophils (as indicated by the *SIGLEC8* gene) compared to healthy controls (HC) (n = 10) (A). Pearson correlation analysis between *FCGRIIIB* and *SIGLEC8* expression and renal function (log2 GFR) in DN patients (n = 16) was also assessed (B).

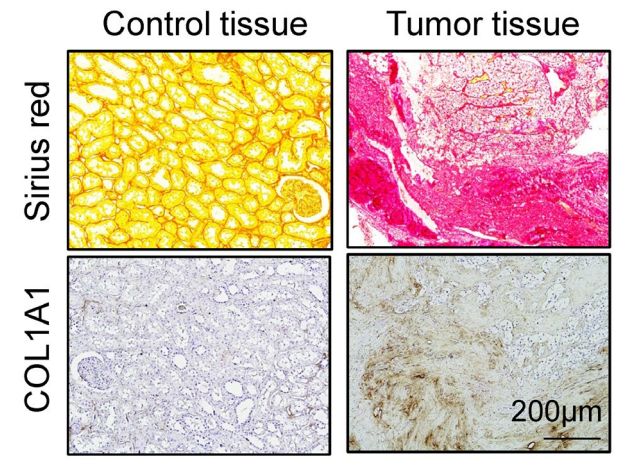


**Figure 53. Fibrotic changes of control and tumor tissues from nephrectomy specimen of RCC patients.**

Sirius-red (upper panel) and COL1A1 immunohistochemistry (lower panel) of tumor or normal lesion from RCC patients.

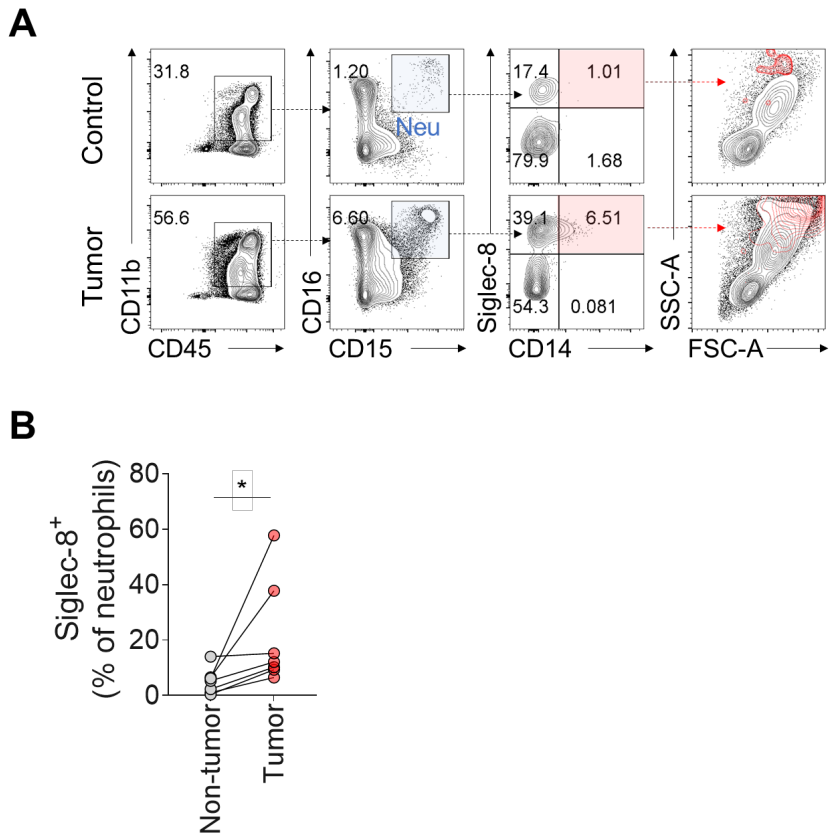


**Figure 54. Siglec-8$^{+}$ neutrophils in human kidney tissues.**

Nephrectomy specimens from seven patients with RCC were subjected to flow cytometry to determine the frequencies of Siglec-8$^{+}$ neutrophils (CD11b$^{+}$CD15$^{+}$CD16$^{+}$ and SSC$^{high}$) in the healthy and tumor counterparts of each specimen. All results are shown as mean ± SEM and statistical analysis was performed using Wilcoxon rank sum test. *$P$<0.05.

# DISCUSSION

Given that neutrophils are the most abundant inflammatory cells in the blood, substantial study has been undertaken on both their protective and harmful functions in a variety of inflammatory and fibrotic disorders[60, 61]. Their involvement in renal fibrosis, however, have received little attention. I report for the first time that ureteral obstruction induces and significantly expands a recently identified Siglec-F-expressing neutrophil subpopulation in the fibrotic kidney. Our subsequent comprehensive characterization of these novel cells revealed that, while they are derived from conventional neutrophils, they are larger and more granular, more likely to be hyper-segmented, and express higher levels of the activation markers CD11b and LRRC32, as well as the effector cytokines TGF-β1, TNF-α, and IL-1β. Furthermore, unlike conventional neutrophils, Siglec-F-expressing neutrophils efficiently drive fibroblasts to generate Collagen 1 via the cytokines produced by the Siglec-F-expressing neutrophils. Notably, I also demonstrate for the first time that these cells produce Collagen 1. This shows that neutrophils expressing Siglec-F contribute to fibrosis through (i) directly generating Collagen 1 and (ii) promoting the production of Collagen 1 by other cells. Additionally, I observed that Siglec-$F^+$ neutrophils were increased in renal fibrosis models with the different disease nature from UUO (i.e., Adriamycin-induced nephropathy and IRI). Additionally, *SIGLEC8*, the human homolog of Siglec-F, is elevated in the renal tissues of DN and FSGS patients when compared to healthy controls, as well as in the fibrotic renal tissues from tumor patients when compared to their healthy renal tissues. Finally, depletion and adoptive transfer of Siglec-$F^+$ neutrophils established their role in renal fibrosis and identified them as possible therapeutic targets.

Because Siglec-F and Ly-6G are eosinophil and neutrophil markers, respectively, our initial tests following the discovery of Siglec-F$^+$ Ly-6G$^+$ cells in fibrotic kidneys determined whether these cells were neutrophil or eosinophil. They were identified as neutrophils because they (i) exhibited the characteristic blue Diff-Quick-stained multilobed nuclei of neutrophils, (ii) co-expressed the neutrophil marker Siglec-E but not the eosinophil marker CCR3, (iii) they were also induced by UUO in ΔdblGATA mice, which cannot generate eosinophils, and (iv) they could be generated in vitro from conventional bone-marrow derived neutrophils.

The first time that Siglec-F$^+$ neutrophils were reported was in a 2017 investigation on tumors[24]. Other investigations have since confirmed their tumor-promoting properties[26, 62]. Additionally, several other inflammatory diseases have been found to induce Siglec-F$^+$ neutrophils, including nasal infection[63], allergic rhinitis[27], asthma[31], and myocardial infarction[29]. Unlike us, tumor studies discovered that Siglec-F$^+$ neutrophils were morphologically identical to conventional neutrophils[24, 26]. Additionally, it appears that the role of Siglec-F$^+$ neutrophils is context-dependent. While Siglec-F$^+$ neutrophils promote tumor growth regardless of the type of tumor[62], they also aid in the healing of inflamed olfactory neuroepithelium[27] and the clearing of *Bordetella pertussis* from the nasal epithelium[63]. While Siglec-F$^+$ neutrophils can be created under a variety of situations, their roles may be altered by the specific stimuli and microenvironments in which they are formed and function. Additional research on the effect of context on Siglec-F$^+$ neutrophil activity is necessary.

I noticed that UUO-treated mice did not have Siglec-F$^+$ neutrophils in their peripheral blood, spleen, or bone marrow. Furthermore, the rapid expansion of the Siglec-F$^+$ neutrophil population in the wounded kidney was accompanied by an

equally rapid expansion of conventional neutrophils in the peripheral blood, spleen, and damaged kidney. This shows that Siglec-$F^+$ neutrophils are formed in the fibrotic kidney from conventional neutrophils in parenchyma or renal vasculature of the injured kidney. Our tests with BV650-CD45 monoclonal antibodies demonstrated that the latter was true. The few Siglec-$F^+$ neutrophils in the healthy kidney were almost entirely concentrated in the renal vasculature in the sham-treated mice. However, following UUO, half of the rapidly increasing Siglec-$F^+$ neutrophil population in the injured kidney was found in the parenchyma, while the remaining half was found in the blood vessels. Given that this pattern persisted 14 days after UUO and that the Siglec-$F^+$ neutrophils in the injured kidney were also low proliferative and apoptotic, it appears that the parenchymal Siglec-$F^+$ neutrophil population is constantly replenished via conversion of conventional neutrophils in the renal vessels, followed by migration of the newly formed Siglec-$F^+$ neutrophils into the renal parenchyma.

Numerous lines of evidence indicate that inflammatory cytokines play a significant role in the onset and progression of CKD[16]. I observed that our UUO-injured kidneys expressed significantly higher levels of TGF-β1, GM-CSF, IL-23, and MCP-1 than sham-treated kidneys. As a result, I hypothesized that the altered cytokine milieu in the kidney might be responsible for the generation of Siglec-$F^+$ neutrophils. Indeed, the levels of these cytokines in the kidney following UUO were positively correlated with Siglec-$F^+$ neutrophil frequencies in the kidney. Additionally, TGF-β1 and GM-CSF promoted the expression of Siglec-F in conventional murine neutrophils and Siglec-8 in naive human neutrophils. Thus, TGF-β1 and, more specifically, GM-CSF induce the conversion of conventional neutrophils to Siglec-$F^+$ neutrophils.

Notably, I discovered that Siglec-F$^+$ neutrophils produced following UUO or priming with TGF-β1 or GM-CSF expressed Collagen 1. Although there are diverse ECM proteins accumulated during fibrosis, type 1 collagen (collagen 1) is one of the major proteins involved in the renal fibrosis. Myofibroblasts are thought to produce the majority of ECM proteins in renal fibrosis[64]. This was recently challenged by Buchtler et al., who examined the extent of renal fibrosis in mice with conditionally knocked-out COL1A1 in CD45$^+$ cells: when these mice were subjected to UUO or adriamycin-induced nephropathy, their renal fibrosis was significantly reduced compared to wildtype mice[55]. Although they did not specify which CD45$^+$ leukocytes produced Collagen 1, they concluded that leukocytes were responsible for 38–50% of Collagen 1 deposition in renal fibrosis. This is supported by a recent study[65] that reanalyzed single-cell RNA sequencing data from UUO-injured kidneys and discovered that immune cells, including neutrophils, express COL1A1 as well as other collagen proteins such as COL5A2, COL12A1, and COL15A1[66]. Our observation that Siglec-F$^+$ neutrophils are the predominant source of Collagen 1 in the fibrotic kidney corroborates and expands on previous findings. Our Siglec-F$^+$ neutrophil mAb depletion tests further support this hypothesis: both anti-Ly-6G and anti-Siglec-F mAbs greatly reduced UUO-induced fibrosis. Notably, whereas both mAbs efficiently suppressed Siglec-F$^+$ neutrophils, the anti-Ly-6G mAb significantly decreased fibrosis compared to the anti-Siglec-F mAb. This could be due to an unexpected rise in eosinophils following anti-Ly-6G treatment, which may have a pro-fibrotic effect. Additional mechanistic research is necessary.

Although the role of neutrophils in renal failure has been relatively understudied to date, a few studies demonstrate unequivocally that they exist and

play a role in glomerulonephritis with a variety of etiologies[67, 68, 69, 70]. The current study confirms and extends previous findings by demonstrating that fibrotic kidneys in both murine and human models induce the new pro-fibrotic Siglec-$F^+$ (mouse) or Siglec-$8^+$ (human) neutrophil. This shows that neutrophil profiling may have clinical utility in patients with renal fibrosis or CKD. Additionally, our studies imply that immunotherapies could be used to target this novel immune cell type, potentially interrupting or reversing the inexorable course of renal fibrosis. To ascertain the clinical relevance of our findings, I need to first confirm the presence of Siglec-8-expressing neutrophils and their features at various phases of renal fibrosis or CKD in large and diverse patient cohorts. Nonetheless, from a pathophysiological standpoint, I hope that the functional analysis and molecular profiling of Siglec-$F^+$ neutrophils described here will contribute to the field's understanding of the micro-inflammatory environment associated with renal fibrosis.

There are still few limitations in this study. First, I showed the role of Siglec-$F^+$ neutrophils in renal fibrosis mostly using the UUO model where the fibrosis is localized in tubulointerstitium. Although the tubulointerstitial fibrosis is the common final destination for all progressive renal diseases even including glomerular diseases, the functional study based on UUO model might not guarantee that Siglec-$F^+$ neutrophils also contribute to the fibrosis in glomerular compartment. The only evidence was the increase of Siglec-$F^+$ neutrophils in the renal IRI model which accompany both glomerular and tubulointerstitial fibrosis. Second, I was unable to quantify the contribution of two pro-fibrotic mechanisms of Siglec-$F^+$ neutrophils to renal fibrosis: is it their production of Collagen 1 that is more important, or is it their production of pro-fibrotic cytokines (which induce

other cells to produce Collagen 1)? The application of a conditional COL1A1 deletion system to neutrophils may provide answers to these questions. Additionally, I have not been able to study renal tissues from individuals with renal fibrosis other than tumor to determine whether they also include Siglec-$8^+$ neutrophils and whether they contribute to fibrosis development. While these investigations are ongoing, they are impeded by the difficulty of acquiring adequate kidney samples from individuals with CKD for flow cytometric examination. Nonetheless, our study is the first to demonstrate the presence of Siglec-$F^+$ neutrophils in the fibrotic kidney. Our comprehensive analysis using a variety of renal fibrosis models, in vitro experiments, and human transcriptomics and tissue experiments also indicates that these cells play a significant role in the fibrotic process and may be targeted therapeutically to promote tissue recovery and slow the progression of renal fibrosis.

# CONCLUSION

In this study, I discovered the role of Siglec-F$^{+}$ neutrophils in the renal inflammation and fibrosis. Given the unmet clinical demands for renal fibrosis, the identification of novel pharmaceutical targets for interfering in disease progression is critical. To identify the key immune cells involved in the renal fibrosis, I aimed to investigate the changes of immune cell landscapes including minor innate immune cells. I identified that the affected kidney included a substantial and rapidly emerging population of neutrophils that showed the eosinophil marker Siglec-F when I examined these cells in the unilateral ureteral obstruction (UUO) mice model of renal fibrosis. I initially determined that they were neutrophils. I then demonstrated that TGF-β1 and GM-CSF derived these cells from conventional neutrophils in the renal vasculature. In addition, they were differed from conventional neutrophils by more frequent hypersegmentation, higher expression of pro-fibrotic and inflammatory cytokines. and, most importantly, expression of collagen 1. I demonstrated their roles in renal fibrosis by the specific depletion and adoptive transfer of Siglec-F$^{+}$ neutrophils **(Figure 55)**. Thus, these studies have uncovered a subgroup of neutrophils that contributes to renal fibrosis and, potentially, a novel therapeutic target for renal fibrosis and/or CKD.

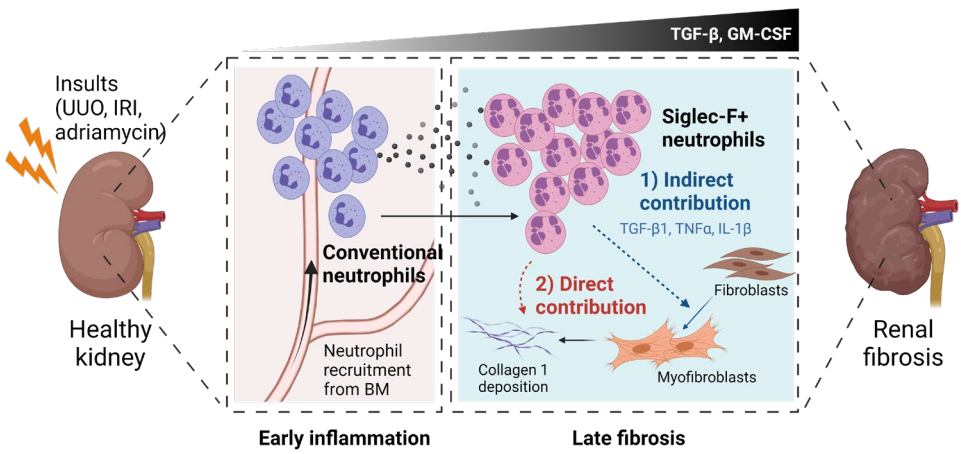


**Figure 55. Graphical summary of this study.**

During renal injury leading to renal fibrosis, conventional neutrophils were infiltrated and conversed to Siglec-$F^{+}$ neutrophils in the injured kidney by TGF-β1 and GM-CSF. The Siglec-$F^{+}$ neutrophils contributed to renal fibrosis via two pathways: direct pathway of producing collagen 1, and indirect pathway of inducing activation of myofibroblasts through TGF-β1, TNF-α, and IL-1β. The figure was created with Biorender.com.

# REFERENCES


1. Ryu, S. *et al.* Siglec-F-expressing neutrophils are essential for creating a profibrotic microenvironment in renal fibrosis. *J Clin Invest* **132** (2022).

2. Kalantar-Zadeh, K., Jafar, T.H., Nitsch, D., Neuen, B.L. & Perkovic, V. Chronic kidney disease. *Lancet* **398**, 786-802 (2021).

3. Chen, T.K., Knicely, D.H. & Grams, M.E. Chronic Kidney Disease Diagnosis and Management: A Review. *JAMA* **322**, 1294-1304 (2019).

4. Breyer, M.D. & Susztak, K. The next generation of therapeutics for chronic kidney disease. *Nat Rev Drug Discov* **15**, 568-588 (2016).

5. Pollock, C. *et al.* The establishment and validation of novel therapeutic targets to retard progression of chronic kidney disease. *Kidney Int Suppl (2011)* **7**, 130-137 (2017).

6. Meng, X.M., Nikolic-Paterson, D.J. & Lan, H.Y. Inflammatory processes in renal fibrosis. *Nat Rev Nephrol* **10**, 493-503 (2014).

7. Stenvinkel, P. *et al.* Chronic Inflammation in Chronic Kidney Disease Progression: Role of Nrf2. *Kidney Int Rep* **6**, 1775-1787 (2021).

8. Zoccali, C., Tripepi, G. & Mallamaci, F. Dissecting inflammation in ESRD: do cytokines and C-reactive protein have a complementary prognostic value for mortality in dialysis patients? *J Am Soc Nephrol* **17**, S169-173 (2006).

9. Amdur, R.L. *et al.* Inflammation and Progression of CKD: The CRIC Study. *Clin J Am Soc Nephrol* **11**, 1546-1556 (2016).

10. Perlman, A.S. *et al.* Serum Inflammatory and Immune Mediators Are Elevated in Early Stage Diabetic Nephropathy. *Ann Clin Lab Sci* **45**, 256-263 (2015).

11. Schroder, K., Sweet, M.J. & Hume, D.A. Signal integration between IFNgamma and TLR signalling pathways in macrophages. *Immunobiology* **211**, 511-524 (2006).

12. Ryu, M. *et al.* Bacterial CpG-DNA accelerates Alport glomerulosclerosis by inducing an M1 macrophage phenotype and tumor necrosis factor-alpha-mediated podocyte loss. *Kidney Int* **79**, 189-198 (2011).

13. Rosin, D.L. & Okusa, M.D. Dangers within: DAMP responses to damage and cell death in kidney disease. *J Am Soc Nephrol* **22**, 416-425 (2011).

14. Gupta, S. & Kaplan, M.J. The role of neutrophils and NETosis in autoimmune and renal diseases. *Nat Rev Nephrol* **12**, 402-413 (2016).

15. Awad, A.S. *et al.* Compartmentalization of neutrophils in the kidney and lung following acute ischemic kidney injury. *Kidney Int* **75**, 689-698 (2009).

16. Lee, S.B. & Kalluri, R. Mechanistic connection between inflammation and fibrosis. *Kidney Int Suppl*, S22-26 (2010).

17. Wynn, T.A. Cellular and molecular mechanisms of fibrosis. *J Pathol* **214**, 199-210 (2008).

18. Burn, G.L., Foti, A., Marsman, G., Patel, D.F. & Zychlinsky, A. The Neutrophil. *Immunity* **54**, 1377-1391 (2021).

19. Mayadas, T.N., Cullere, X. & Lowell, C.A. The multifaceted functions of neutrophils. *Annu Rev Pathol* **9**, 181-218 (2014).

20. Ng, L.G., Ostuni, R. & Hidalgo, A. Heterogeneity of neutrophils. *Nat Rev Immunol* **19**, 255-265 (2019).

21. Hong, C.W. Current Understanding in Neutrophil Differentiation and Heterogeneity. *Immune Netw* **17**, 298-306 (2017).

22. Fridlender, Z.G. *et al.* Polarization of tumor-associated neutrophil phenotype by TGF-beta: "N1" versus "N2" TAN. *Cancer Cell* **16**, 183-194 (2009).

23. Xie, X. *et al.* Single-cell transcriptome profiling reveals neutrophil heterogeneity in homeostasis and infection. *Nat Immunol* **21**, 1119-1133 (2020).

24. Engblom, C. *et al.* Osteoblasts remotely supply lung tumors with cancer-promoting SiglecF(high) neutrophils. *Science* **358** (2017).

25. Rosenberg, H.F., Dyer, K.D. & Foster, P.S. Eosinophils: changing perspectives in health and disease. *Nat Rev Immunol* **13**, 9-22 (2013).

26. Pfirschke, C. *et al.* Tumor-Promoting Ly-6G(+) SiglecF(high) Cells Are Mature and Long-Lived Neutrophils. *Cell Rep* **32**, 108164 (2020).

27. Ogawa, K. *et al.* Frontline Science: Conversion of neutrophils into atypical Ly6G(+) SiglecF(+) immune cells with neurosupportive potential in olfactory neuroepithelium. *J Leukoc Biol* **109**, 481-496 (2021).

28. Borkner, L., Curham, L.M., Wilk, M.M., Moran, B. & Mills, K.H.G. IL-17 mediates protective immunity against nasal infection with Bordetella pertussis by mobilizing neutrophils, especially Siglec-F(+) neutrophils.

*Mucosal Immunol* **14**, 1183-1202 (2021).

29. Vafadarnejad, E. *et al.* Dynamics of Cardiac Neutrophil Diversity in Murine Myocardial Infarction. *Circ Res* **127**, e232-e249 (2020).

30. Calcagno, D.M. *et al.* SiglecF(HI) Marks Late-Stage Neutrophils of the Infarcted Heart: A Single-Cell Transcriptomic Analysis of Neutrophil Diversification. *J Am Heart Assoc* **10**, e019019 (2021).

31. Shin, J.W. *et al.* A unique population of neutrophils generated by air pollutant-induced lung damage exacerbates airway inflammation. *J Allergy Clin Immunol* (2021).

32. Kular, J.K., Basu, S. & Sharma, R.I. The extracellular matrix: Structure, composition, age-related differences, tools for analysis and applications for tissue engineering. *J Tissue Eng* **5**, 2041731414557112 (2014).

33. Bulow, R.D. & Boor, P. Extracellular Matrix in Kidney Fibrosis: More Than Just a Scaffold. *J Histochem Cytochem* **67**, 643-661 (2019).

34. Herrera, J., Henke, C.A. & Bitterman, P.B. Extracellular matrix as a driver of progressive fibrosis. *J Clin Invest* **128**, 45-53 (2018).

35. Gerarduzzi, C. & Di Battista, J.A. Myofibroblast repair mechanisms post-inflammatory response: a fibrotic perspective. *Inflamm Res* **66**, 451-465 (2017).

36. Tampe, D. & Zeisberg, M. Potential approaches to reverse or repair renal fibrosis. *Nat Rev Nephrol* **10**, 226-237 (2014).

37. Mack, M. & Yanagita, M. Origin of myofibroblasts and cellular events triggering fibrosis. *Kidney Int* **87**, 297-307 (2015).

38. Liu, Y. Cellular and molecular mechanisms of renal fibrosis. *Nat Rev Nephrol* **7**, 684-696 (2011).

39. Anderson, K.G. *et al.* Intravascular staining for discrimination of vascular and tissue leukocytes. *Nat Protoc* **9**, 209-222 (2014).

40. Chevalier, R.L., Forbes, M.S. & Thornhill, B.A. Ureteral obstruction as a model of renal interstitial fibrosis and obstructive nephropathy. *Kidney Int* **75**, 1145-1152 (2009).

41. Johnston, L.K. & Bryce, P.J. Understanding Interleukin 33 and Its Roles in Eosinophil Development. *Front Med (Lausanne)* **4**, 51 (2017).

42. Zoccali, C. *et al.* The systemic nature of CKD. *Nat Rev Nephrol* **13**, 344-358 (2017).

43. Deniset, J.F. & Kubes, P. Neutrophil heterogeneity: Bona fide subsets or polarization states? *J Leukoc Biol* **103**, 829-838 (2018).

44. Tateno, H., Crocker, P.R. & Paulson, J.C. Mouse Siglec-F and human Siglec-8 are functionally convergent paralogs that are selectively expressed on eosinophils and recognize 6'-sulfo-sialyl Lewis X as a preferred glycan ligand. *Glycobiology* **15**, 1125-1135 (2005).

45. Tapmeier, T.T. *et al.* Pivotal role of CD4+ T cells in renal fibrosis following ureteric obstruction. *Kidney Int* **78**, 351-362 (2010).

46. McGeachy, M.J. & Cua, D.J. T cells doing it for themselves: TGF-beta regulation of Th1 and Th17 cells. *Immunity* **26**, 547-549 (2007).

47. McGeachy, M.J. GM-CSF: the secret weapon in the T(H)17 arsenal. *Nat Immunol* **12**, 521-522 (2011).

48. Xu, L., Sharkey, D. & Cantley, L.G. Tubular GM-CSF Promotes Late MCP-1/CCR2-Mediated Fibrosis and Inflammation after Ischemia/Reperfusion Injury. *J Am Soc Nephrol* **30**, 1825-1840 (2019).

49. Qi, R. & Yang, C. Renal tubular epithelial cells: the neglected mediator of tubulointerstitial fibrosis after injury. *Cell Death Dis* **9**, 1126 (2018).

50. Silvestre-Roig, C., Hidalgo, A. & Soehnlein, O. Neutrophil heterogeneity: implications for homeostasis and pathogenesis. *Blood* **127**, 2173-2181 (2016).

51. Geng, S., Zhang, Y., Lee, C. & Li, L. Novel reprogramming of neutrophils modulates inflammation resolution during atherosclerosis. *Sci Adv* **5**, eaav2309 (2019).

52. Stockis, J., Dedobbeleer, O. & Lucas, S. Role of GARP in the activation of latent TGF-beta1. *Mol Biosyst* **13**, 1925-1935 (2017).

53. Sahai, E. *et al.* A framework for advancing our understanding of cancer-associated fibroblasts. *Nat Rev Cancer* **20**, 174-186 (2020).

54. Van Linthout, S., Miteva, K. & Tschope, C. Crosstalk between fibroblasts and inflammatory cells. *Cardiovasc Res* **102**, 258-269 (2014).

55. Buchtler, S. *et al.* Cellular Origin and Functional Relevance of Collagen I Production in the Kidney. *J Am Soc Nephrol* **29**, 1859-1873 (2018).

56. Nikolic-Paterson, D.J., Wang, S. & Lan, H.Y. Macrophages promote renal fibrosis through direct and indirect mechanisms. *Kidney Int Suppl (2011)* **4**, 34-38 (2014).

57. Lee, V.W. & Harris, D.C. Adriamycin nephropathy: a model of focal

segmental glomerulosclerosis. *Nephrology (Carlton)* **16**, 30-38 (2011).

58. Fu, Y. *et al.* Rodent models of AKI-CKD transition. *Am J Physiol Renal Physiol* **315**, F1098-F1106 (2018).

59. Joung, J.W., Oh, H.K., Lee, S.J., Kim, Y.A. & Jung, H.J. Significance of Intratumoral Fibrosis in Clear Cell Renal Cell Carcinoma. *J Pathol Transl Med* **52**, 323-330 (2018).

60. Nemeth, T., Sperandio, M. & Mocsai, A. Neutrophils as emerging therapeutic targets. *Nat Rev Drug Discov* **19**, 253-275 (2020).

61. Kolahian, S., Fernandez, I.E., Eickelberg, O. & Hartl, D. Immune Mechanisms in Pulmonary Fibrosis. *Am J Respir Cell Mol Biol* **55**, 309-322 (2016).

62. Veglia, F. *et al.* Analysis of classical neutrophils and polymorphonuclear myeloid-derived suppressor cells in cancer patients and tumor-bearing mice. *J Exp Med* **218** (2021).

63. Borkner, L., Curham, L.M., Wilk, M.M., Moran, B. & Mills, K.H.G. IL-17 mediates protective immunity against nasal infection with Bordetella pertussis by mobilizing neutrophils, especially Siglec-F(+) neutrophils. *Mucosal Immunol* (2021).

64. Duffield, J.S. Cellular and molecular mechanisms in kidney fibrosis. *J Clin Invest* **124**, 2299-2306 (2014).

65. Conway, B.R. *et al.* Kidney Single-Cell Atlas Reveals Myeloid Heterogeneity in Progression and Regression of Kidney Disease. *J Am Soc Nephrol* **31**, 2833-2854 (2020).

66. Schmidt, I.M. *et al.* Cadherin-11, Sparc-related modular calcium binding protein-2, and Pigment epithelium-derived factor are promising non-invasive biomarkers of kidney fibrosis. *Kidney Int* **100**, 672-683 (2021).

67. Hooke, D.H., Gee, D.C. & Atkins, R.C. Leukocyte analysis using monoclonal antibodies in human glomerulonephritis. *Kidney Int* **31**, 964-972 (1987).

68. Sorger, K. *et al.* Subtypes of acute postinfectious glomerulonephritis. Synopsis of clinical and pathological features. *Clin Nephrol* **17**, 114-128 (1982).

69. Kincaid-Smith, P., Nicholls, K. & Birchall, I. Polymorphs infiltrate glomeruli in mesangial IgA glomerulonephritis. *Kidney Int* **36**, 1108-1111 (1989).

70. Camussi, G. *et al.* The polymorphonuclear neutrophil (PMN)

immunohistological technique: detection of immune complexes bound to the PMN membrane in acute poststreptococcal and lupus nephritis. *Clin Nephrol* **14**, 280-287 (1980).

국문초록

# Siglec-F 발현 호중구에 의한 신장 섬유화 병인 기전 연구

서울대학교 대학원

의과학과 의과학전공

류승원

신장질환에서 조직 내 염증은 흔하게 동반되어 있으며, 신장질환의 진행에 중요한 역할을 하는 것으로 알려져 있음. 만성적인 신장 손상 및 염증은 조직 내 섬유화를 유발하게 되며 신장 기능의 비가역적인 저하를 유발하게 됨. 신장 섬유화의 대한 근본적인 치료제는 존재하지 않으며, 신장 기능 저하에 따른 투석이나 신장 이식이 필요한 신부전으로의 진행을 예방하기 위해 기저 원인을 조절하는 전략이 이용되고 있음. 현재까지 신장 면역 반응 연구는 특정 면역세포에 집중되어 진행되었기 때문에, 조직 내 작은 수를 차지하는 선천면역세포의 역할에 대해서는 잘 다루어지지 않았음. 본 연구자는 이러한 이전까지 역할이 잘 알려지지 않았던 선천면역세포의 기능을 위주로 신장 질환에서 동반되

는 염증과 섬유화 기전을 이해함으로써, 해당 병리 기전 제어를 통한 신장 질환의 치료법 제시를 기대하였음.

이를 위해, 단측요관 폐색을 통한 신장 섬유화 동물 모델을 사용하여 동반되는 염증 반응에서 중성구에 의한 역할에 대해 연구함. 신장 섬유화의 증가에 따라 중성구의 수가 현저하게 증가함. 이 때 신장 조직에서 증가하는 중성구의 약 절반 정도에서 Siglec-F를 발현함. Siglec-F는 주로 호산구에서 발현되어 호산구의 존재를 확인할 때 이용되는 핵심 마커인데, 최근 암이나 천식과 같은 염증 상황에서 Siglec-F를 발현하고 있는 중성구가 나타날 수 있음이 보고된 바 있었음. 신장 섬유화가 진행되는 과정에서 나타난 Siglec-F 발현 중성구는 오직 염증이 유도된 신장 내에서만 발견되어, 신손상이 일어난 환경 내에서 특이적으로 유도됨을 확인함. 해당 특이 중성구는 일반적인 중성구에 비해 염증성 사이토카인을 더 높게 발현하며, 성숙된 형태인 과분절된 형태로 관찰됨. Siglec-F 발현 호중구를 신장 섬유화 모델에 도입하거나 선택적으로 없애는 실험을 통해, 해당 세포가 신장 염증 및 섬유화에 핵심적인 세포임을 확인함. 신손상 조직에서 발견된 이 세포는 사이토카인 분비를 통해 간접적으로 섬유화에 기여할 뿐만 아니라, 직접 세포외기질인 콜라겐 단백질을 발현함으로써 섬유화에 기여할 수 있음을 제시함. 이러한 특정 섬유화 유도 모델에서 발견된 Siglec-F 발현 중성구의 역할이 다른 기전에 매개한 섬유화 모델에서도 동일하게 나타날 수 있는지 확인하고자 다른 신장 섬유화 동물 모델(Adriamycin 유도 신손상 및 신장 허혈-재관류 손상 모델)에서도 Siglec-F 발현 중성구의 증가를 확인함. 또한 섬유화가 동반되어 있는 신세포암 환자의 적출된 암 조직에서 Siglec-8 발현 중성구의 증가를 확인함으로써, 새롭게 발견된 중성구의 아형이 사람 신장 조직의

섬유화에도 기여할 가능성을 확인함.

본 연구자는 학위과정 동안 이전까지 신장에서 연구되지 않았던 새로운 아형의 중성구에 의한 염증 반응 및 섬유화 기전에 대해 연구하였음. 섬유화의 핵심 병인 면역세포로써 Siglec-F 발현 중성구에 대한 연구를 통해, 이전까지 관심이 부족하였던 신장의 선천면역세포의 기능 조절을 통한 신장질환의 치료에 새로운 전략을 제공할 것으로 기대됨.

주요어: 신장염, 신장 섬유화, 선천면역, 호중구

학번: 2017-39911